2019

Long-term correction of hemophilia B using adenoviral delivery of CRISPR/Cas9

Calvin J. Stephens
Washington University School of Medicine in St. Louis

Elvin J. Lauron
Washington University School of Medicine in St. Louis

Elena Kashentseva
Washington University School of Medicine in St. Louis

Zhi Hong Lu
Washington University School of Medicine in St. Louis

Wayne M. Yokoyama
Washington University School of Medicine in St. Louis

See next page for additional authors

Journal of Controlled Release 298 (2019) 128–141

Contents lists available at ScienceDirect

Journal of Controlled Release

journal homepage: www.elsevier.com/locate/jconrel

Long-term correction of hemophilia B using adenoviral delivery of CRISPR/Cas9

Calvin J. Stephens[a,b], Elvin J. Lauron[c], Elena Kashentseva[a], Zhi Hong Lu[a], Wayne M. Yokoyama[c], David T. Curiel[a,d,*]

[a] Cancer Biology Division, Department of Radiation Oncology, Washington University School of Medicine, 660 South Euclid Avenue, Campus Box 8224, St. Louis, MO 63110, USA
[b] Molecular Genetics and Genomics Program, Division of Biology and Biomedical Sciences, Washington University School of Medicine, 660 South Euclid Avenue, Campus Box 8226, St. Louis, MO 63110, USA
[c] Division of Rheumatology, Department of Medicine, Washington University School of Medicine, 660 South Euclid Avenue, Campus Box 8045, St. Louis, MO 63110, USA
[d] Department of Radiation Oncology, Biologic Therapeutics Center, Washington University School of Medicine, 660 South Euclid Avenue, Campus Box 8224, St. Louis, MO 63110, USA

ARTICLE INFO

Keywords:
Gene therapy
Gene editing
CRISPR/Cas9
Hemophilia
Adenovirus

ABSTRACT

Hemophilia B (HB) is a life-threatening inherited disease caused by mutations in the *FIX* gene, leading to reduced protein function and abnormal blood clotting. Due to its monogenic nature, HB is one of the primary targets for gene therapy. Indeed, successful correction of HB has been shown in clinical trials using gene therapy approaches. However, application of these strategies to non-adult patients is limited due to high cell turnover as young patients develop, resulting in vector dilution and subsequent loss of therapeutic expression. Gene editing can potentially overcome this issue by permanently inserting the corrective gene. Integration allows replication of the therapeutic transgene at every cell division and can avoid issues associated with vector dilution. In this study, we explored adenovirus as a platform for corrective CRISPR/Cas9-mediated gene knock-in. We determined as a proof-of-principle that adenoviral delivery of CRISPR/Cas9 is capable of corrective gene addition, leading to long-term augmentation of FIX activity and phenotypic correction in a murine model of juvenile HB. While we found on-target error-free integration in all examined samples, some mice also contained mutations at the integration target site. Additionally, we detected adaptive immune responses against the vector and Cas9 nuclease. Overall, our findings show that the adenovirus platform is suitable for gene insertion in juveniles with inherited disease, suggesting this approach may be applicable to other diseases.

1. Introduction

Recent clinical trials have shown success in treatment of inherited genetic diseases with gene therapy owing to sustained therapeutic gene expression. In particular, gene therapies for hemophilia B (HB) have attained long-term disease correction in human patients using recombinant adeno-associated viral (rAAV) vectors [1–3]. HB is a life-threatening inherited disease caused by mutations in the coagulation Factor IX (FIX) gene. These mutations lead to absent or aberrant FIX function within the blood coagulation cascade, characterized by the inability to form proper blood clots. Due to its monogenic nature, HB is a preeminent target for gene therapy. Although effective in liver-directed gene transfer for adults, current gene replacement therapies are inadequate for application in pediatric and young patients, based upon preclinical findings in non-adult animals [4–7]. In non-adult animal models, gene expression decreases over time for several reasons including vector dilution and the loss of transduced cell populations. In non-adults, transferred episomal genes dilute from cell division during liver growth, in contrast to quiescent adult livers [4–7]. In both adults and non-adults the loss of transduced cell populations can also limit therapeutic gene expression. Taken together, there remains an unmet need for methods to attain life-long gene expression in pediatric patients. Gene editing is a promising method that may allow for the permanent incorporation of corrective genes into the chromosomes of young patients to overcome loss of gene expression due to vector dilution. Theoretically, such integration may also counteract the loss of transduced cell populations if progenitor or stem cells genetically incorporate the corrective transgene and are not eliminated.

* Corresponding author at: Cancer Biology Division, Department of Radiation Oncology, Washington University School of Medicine, 660 South Euclid Avenue, Campus Box 8224, St. Louis, MO 63110, USA.
E-mail address: dcuriel@wustl.edu (D.T. Curiel).

https://doi.org/10.1016/j.jconrel.2019.02.009
Received 9 November 2018; Received in revised form 28 January 2019; Accepted 8 February 2019
Available online 13 February 2019

Targetable editing-based genomic integration approaches could be exceptionally useful for *in vivo* somatic therapy, with the potential to circumvent the loss of gene expression associated with episomal persistence-based vectors. Such integration allows corrective gene addition or *in situ* correction of the endogenous defective gene. In this regard, lentiviral vectors (LVs) integrate with viral integrases and have achieved sustained gene expression in severely immunodeficient pediatric patients [8–9]. However, integrase-mediated integration occurs promiscuously throughout the genome of target cells, with a preference for transcriptionally active regions, and consequently can perturb the surrounding genomic environment [10–13]. As such, targeting integration to a specific well-characterized locus, termed 'safe harbor', or to endogenous disease loci, is highly desirable. Gene delivery methods using rAAVs have shown targeted gene editing is a plausible strategy to treat models of inherited diseases, including neonatal HB [14–17]. Indeed, rAAV is currently the preferred platform for liver-directed therapies to correct monogenic diseases, including its use in a recent gene editing clinical trial utilizing zinc finger nucleases (ZFN) to treat adult HB [18]. Despite such promising progress, this delivery system has limitations. Of note, random viral integration constitutes the basis of residual rAAV vector persistence after administration in prenatal and neonatal animals and may thus affect residual gene expression levels in developing organisms [5,15,and 19]. Furthermore, the risk associated with random integration of rAAV vector sequences, insertion of vector genomes at editing target sites, and a limited packaging capacity constrain application of this vector in some contexts [20–22].

In contrast, the use of adenovirus vectors to mediate editing-based integration has not been explored to the same degree as rAAVs [23–24]. Adenoviral vectors have a large packaging capacity, which may be useful for integration of large genes or useful for elaborate gene editing strategies [23–27]. Additionally, adenoviral vectors are capable of highly efficient cell-specific infection and do not readily integrate into host genomes [28]. Thus, the use of adenoviral-mediated gene transfer for editing-based integration could accomplish disease correction with reduced genotoxic risk. Nonetheless, whether adenoviral delivery of gene editing systems can overcome the issues which counteract longevity of episomal-based expression has yet to be determined. In other words, any virally transduced cell can encounter vector silencing, immune-mediated elimination, or other mechanisms (such as cell death or high cell turnover) leading to the loss of gene expression- irrespective of whether editing has occurred. Although we have previously shown adenovirus-mediated gene knock-in can augment levels of a serum protein, it remains unclear whether such approach can attain prolonged phenotypic correction in a pediatric disease context [29].

In this study, CRISPR/Cas9 is used to mediate targeted gene integration *in vivo*. Briefly, CRISPR/Cas9 systems use small RNAs to guide an endonuclease to specific DNA sequences and has been applied for a wide variety of therapeutic applications [30]. Adenoviral delivery of CRISPR/Cas9 may have several advantages, including repair accuracy and the size of constructs which may be delivered is greater than other approaches [31]. Herein we explored whether adenoviral vectors could (i) deliver CRISPR/Cas9 to mediate corrective gene knock-in at the *ROSA26* safe harbor locus, (ii) if such editing affects longevity of therapeutic gene expression in a murine model of HB, and (iii) explore vector fate, integration characteristics, and host responses to this strategy. Using this approach, we found a single injection of adenoviral vectors achieved *mFIX* cDNA knock-in at the *ROSA26* safe harbor and long-term phenotypic correction of the HB bleeding diathesis. We determined on-target integrated *mFIX* cDNA was detectable 245 days post-injection (dpi) with errorless and error-containing integration events. Although we detected adaptive immune responses to the adenoviral vector and the Cas9 nuclease, the immunological responses described herein did not abolish therapeutic benefits provided by gene editing. Overall, we demonstrate that adenoviral vectors are capable of targeted gene integration and long-term correction of an inherited disease in juvenile mice. Our findings support the use of gene editing to achieve prolonged gene expression in pediatric patients.

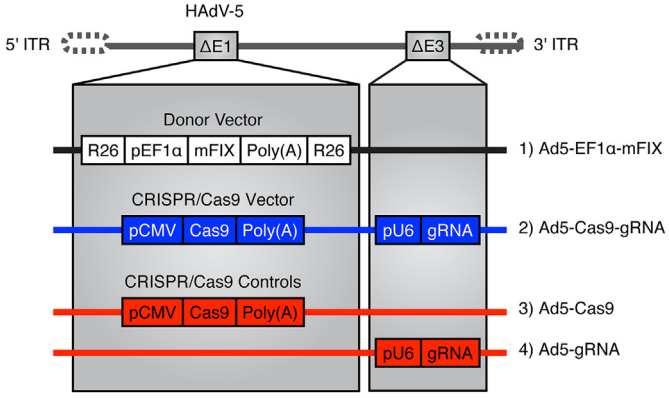

Fig. 1. A schematic of the adenoviral vectors used in this study. Ad5-EF1α-mFIX (vector 1) expresses mFIX under control of the EF1α promoter and provides a homology-directed repair template, allowing gene knock-in. Ad5-EF1α-mFIX consists of ~800 bp of *ROSA26* homology sequences (R26) which flank the genomic target cut site, with the *mFIX* cDNA expression cassette between the homology arms. Ad5-Cas9-gRNA (vector 2) expresses a *ROSA26*-specific gRNA and Cas9 nuclease, to induce double-stranded breaks at the target site. Control vectors for CRISPR/Cas9-mediated integration were vectors expressing either Cas9 (Ad5-Cas9, vector 3) or gRNA (Ad5-gRNA, vector 4) alone.

2. Results

2.1. Adenoviral vector-mediated integration maintains higher levels of mFIX protein than standard non-editing vectors in a hemophilia model

In this study, an adenoviral vector (Ad5-Cas9-gRNA) facilitates gene delivery of the *Streptococcus pyogenes (sp)* Cas9 nuclease and a guide RNA (gRNA) specific to the murine *ROSA26* 'safe harbor', as characterized in a previous study (Fig. 1) [29]. A second vector was constructed for this study, Ad5-EF1α-mFIX, which provides a template for double stranded break (DSB) DNA repair (Fig. 1). Co-injection of Ad5-Cas9-gRNA and Ad5-EF1α-mFIX targets Cas9 to *ROSA26* for DSB generation and subsequent DNA repair (Fig. 2A). After systemic injection with these vectors to facilitate gene transfer of the editing system, we tracked mFIX protein expression in juvenile R333Q hemophilia mice. As Ad5-EF1α-mFIX contains the exogenous EF1α promoter, some mFIX is derived by episomal-based expression from the adenoviral genome. To ascertain mFIX protein expression from residual episomal persistence, we compared Ad5-Cas9 (a non-editing vector lacking a gRNA) (Supplemental Fig. 1) and Ad5-EF1α-mFIX in parallel to the integration-mediating vectors Ad5-Cas9-gRNA and Ad5-EF1α-mFIX. This comparative analysis allows exploration of whether targeted integration of *mFIX* affects temporal expression, in the context of developing mice.

We tail vein injected juvenile mice with equal amounts of Ad5-EF1α-mFIX plus Ad5-Cas9-gRNA or Ad5-Cas9. Each group injection consisted of a 3:1 mix of Ad5-EF1α-mFIX to secondary virus. Plasma from mice was drawn one week before and after injection. Plasma dilutions' ELISA OD-values were greater post-injection compared to plasma taken prior to injection, indicating successful expression, secretion, and detection of mFIX (Supplemental Fig. 1). Upon confirming *in vivo* expression, we tracked mFIX plasma levels of injected mice for 238 days (Fig. 2B). At seven days post-injection (dpi), differences in mFIX expression between Ad5-Cas9-gRNA and Ad5-Cas9 treated mice were not statistically different, supporting the concept that equal amounts of mFIX-expressing virus were delivered to mice. Decreasing mFIX protein expression was noted in all mice during the first 80 days following treatment, with a greater loss of expression in Ad5-Cas9 (non-editing) treated mice, after which protein levels generally stabilized.

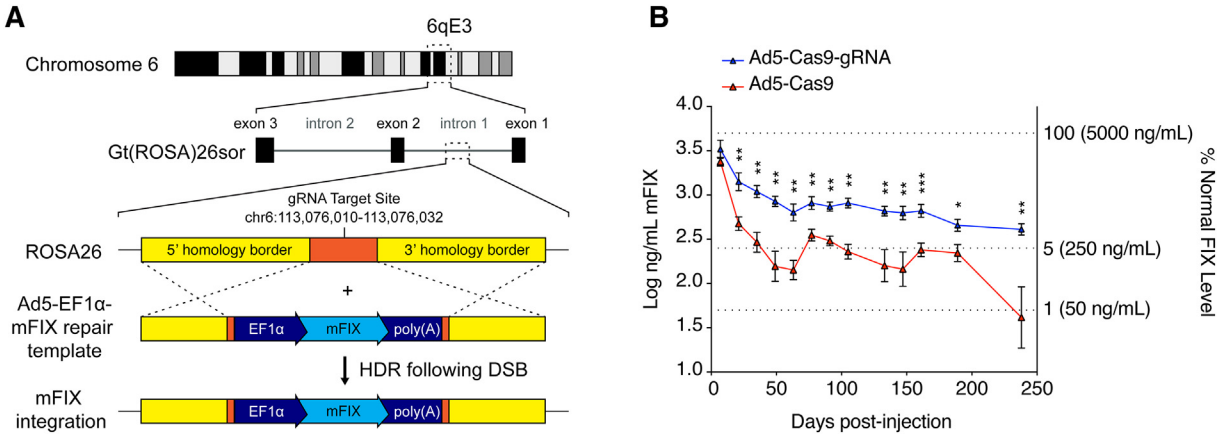

Fig. 2. Knock-in and non-editing adenoviral-based mFIX protein expression in juvenile hemophilia mice. (A) The *ROSA26* locus is targeted by Ad5-Cas9-gRNA to generate a double-stranded break (DSB). The DSB can subsequently be repaired by non-homologous end joining (NHEJ) or homology-directed repair (HDR) when a repair template, such as Ad5-EF1α-mFIX, is present. HDR results in the insertion of the mFIX expression cassette. (B) Four-week old R333Q hemophilia mice were tail vein injected with 7.5×10^{10} viral particles (VP) of Ad5-EF1α-mFIX and 2.5×10^{10} VP of either Ad5-Cas9-gRNA (blue) ($n = 9$) or Ad5-Cas9 (red) ($n = 7$), lacking a gRNA needed for site specific editing. Plasma was drawn intermittently over a 238 day period and concentrations of mFIX determined using ELISA. The right *y*-axis shows FIX activity seen in humans relative to protein levels on the left. Between 50% and 5.0% normal level is considered 'mild' hemophilia, 1–5% normal is the range of 'moderate' hemophilia, while < 1.0% normal represents a 'severe' hemophilia phenotype. Mean values of groups are plotted with error bars denoting SEM. Differences were considered significant with *p*-values of < 0.05, represented by * for values 0.05 to 0.01, 0.01 and 0.001 were denoted by **, and *p*-values < 0.001 by ***. Statistical analysis was performed by parametric (Student's *t*-test or Welch's *t*-test depending on data variance) and non-parametric (Mann-Whitney *U*) testing at individual time points. (For interpretation of the references to colour in this figure legend, the reader is referred to the web version of this article.)

Table 1
Average mFIX plasma levels following adenoviral-mediated gene delivery. The average plasma levels of mFIX (ng/mL), as determined by ELISA, are listed according to days post-injection of four week-old R333Q mice with 7.5×10^{10} VP of Ad5-EF1a-mFIX and 2.5 x 10^{10} VP of either Ad5-Cas9 (left group, $n = 7$) or Ad5-Cas9-gRNA (right group, $n = 9$). SD is standard deviation and SEM is standard error of the mean.

Day post-injection	mFIX ELISA values					
	Ad5-EF1α-mFIX			Ad5-EF1α-mFIX		
	Ad5-Cas9			Ad5-Cas9-gRNA		
	Mean (ng/mL)	SD	SEM	Mean (ng/mL)	SD	SEM
7	2463.3	573.3	216.7	3804.4	1966.9	655.6
21	522.3	240.1	90.74	1581.9	899.8	299.9
35	354.8	224.9	85.01	1103.8	468.5	156.2
49	249.5	244.5	92.39	848.8	352.4	117.5
63	172.9	132.1	53.94	710.2	450.4	150.1
77	381.1	160.3	60.59	857.2	371.9	123.9
91	320.1	122.3	46.22	729.4	283.6	94.5
105	256.4	129.1	48.80	817.3	298.5	99.5
133	230.2	145.8	55.10	659.8	236.7	78.9
147	201.9	100.6	38.03	668.7	324.2	108.1
161	263.3	115.4	43.60	681.2	158.9	91.7
189	252.6	119.6	45.22	471.3	194.7	64.88
238	88.57	64.17	26.19	419.4	134.8	44.93

Moreover, from days 49 to 161, mFIX plasma levels of Ad5-Cas9-gRNA treated mice (the *mFIX* knock-in group) stabilized around 700 ng/mL to 850 ng/mL (Table 1). Over the same period, control Ad5-Cas9 treated mice (non-editing group) exhibited mFIX levels between 200 ng/mL to 350 ng/mL. An important difference between these two approaches was highlighted by the comparison of mFIX levels in treated hemophilia mice to normal human FIX levels (normal ~5000 ng/mL) [14]. Seven days after a single injection, the mFIX plasma levels of all injected mice were within the 'mild' hemophilia range of normal FIX levels (5.0% to 50.0%). Shortly thereafter, some mice treated with the combination of Ad5-EF1α-mFIX and Ad5-Cas9 entered the plasma concentration range of a 'moderate' hemophilia phenotype (1 to 5% normal), as early as 49 dpi (ranging from 1.9% to 17%). Indeed, the average mFIX plasma level of this group was significantly lower than Ad5-EF1α-mFIX and Ad5-Cas9-gRNA knock-in treatment at all time points, excluding seven dpi, for the entirety of the study. Of note, treatment with non-editing vectors led to plasma mFIX levels ranging within or near 'moderate' hemophilia for most of the experiment and dropped into the range of 'severe' hemophilia FIX levels (< 1.0%) by the conclusion of the experiment. This finding represents the reported transient nature of expression from early generation adenoviral vectors.

In total, mice treated with Ad5-Cas9-gRNA along with repair template vector Ad5-EF1α-mFIX (the *mFIX* knock-in group), maintained significantly higher plasma concentrations of mFIX than Ad5-Cas9 (non-editing group) counterparts throughout the time-course, despite receiving equal amount of mFIX-expressing and total virus (Fig. 2B). At 238 dpi, the final mFIX levels in mice treated with Ad5-Cas9-gRNA (*mFIX* knock-in group) averaged 419 ng/mL, representing a maintenance of 11% of the initial expression at seven dpi. In contrast, final mFIX levels in mice administered non-editing Ad5-Cas9 averaged 88.5 ng/mL, representing residual preservation of only 3.5% initial expression. Thus, higher and prolonged therapeutic protein concentrations were provided by integration-mediating vectors in comparison to non-editing vectors, resulting in maintenance of mFIX levels comparative to 'mild' hemophilia phenotypes for the entirety of the experiment.

2.2. *Treatment with integration-mediating vectors provides superior long-term phenotypic correction compared to treatment with non-editing vectors*

To assay disease correction, we performed two experiments at the conclusion of the time-course. First, quantification of FIX enzymatic activity showed a significant improvement between treatment with Ad5-EF1α-mFIX and Ad5-Cas9-gRNA rather than with Ad5-Cas9, in plasma samples taken 238 and 245 dpi (Fig. 3A). Results between these two time points and blood collection sites did not show any meaningful differences (Supplemental Fig. 2). The chromogenic-based measurements of plasma FIX activity showed untreated R333Q hemophiliac mice had nearly undetectable activity (< 1% normal). Plasma from Ad5-Cas9 treated mice showed low residual FIX activity averaging slightly over 1.0% normal, with a maximum of 4.1% normal activity. In

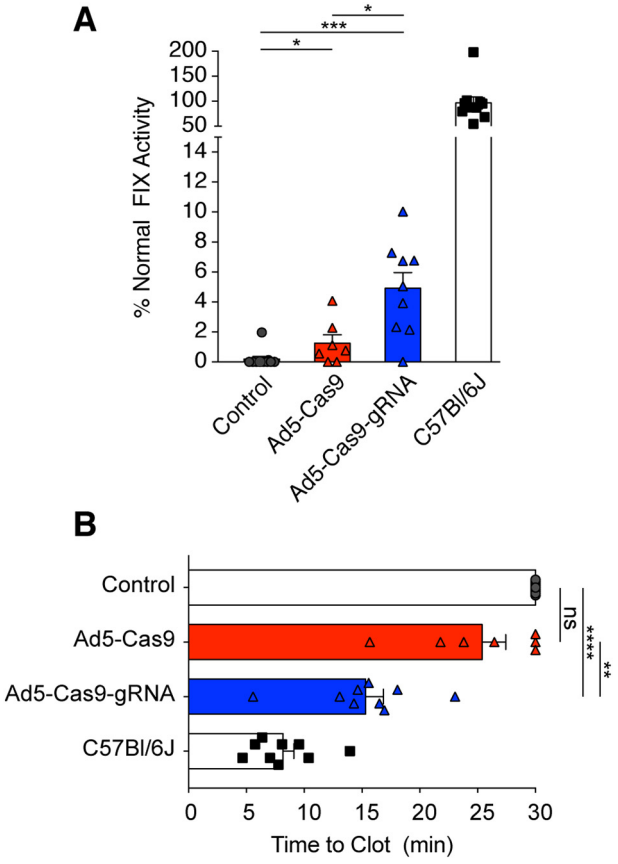

Fig. 3. FIX enzymatic activity in plasma samples and a bleeding assay for functional correction of hemophilia. (A) At the end of the time course, plasma samples from treated and untreated control mice were collected into 3.8% sodium citrate. Plasma dilutions were used in a chromogenic assay to measure FIX enzymatic activity. 100% normal FIX activity was defined by pooled plasma from wild-type C57Bl/6J mice. Plasma was drawn from other C57Bl/6J (n = 10, black squares) and untreated control R333Q hemophilia mice (n = 9, gray circles). Additionally, plasma from mice treated with Ad5-EF1α-mFIX and Ad5-Cas9-gRNA (n = 9, blue triangles) or Ad5-Cas9 (n = 7, red triangles) (control lacking a gRNA) were also tested. Plasma samples from vector-treated mice contained significantly greater FIX activity than untreated R333Q mice (p-value = 0.0353 for Ad5-Cas9, p-value = 0.0003 for Ad5-Cas9-gRNA). Additionally, *mFIX* knock-in treatment using Ad5-Cas9-gRNA significantly increased FIX activity compared to the non-editing Ad5-Cas9 treatment (p-value = 0.0128). Data shown is from three independent tests. Error bars represent SEM. (B) Treated and untreated animal tails were clipped and the time until bleeding had stopped was measured. Differences in bleed time between R333Q control untreated and Ad5-Cas9 (non-editing) treatment were not significant (p-value = 0.0645). Bleed times differed significantly between control untreated and Ad5-Cas9-gRNA (*mFIX* knock-in) treated mice (p-value ≤ 0.0001). Ad5-Cas9-gRNA treated mice also bled significantly less than Ad5-Cas9 treated mice (p-value = 0.0013). (For interpretation of the references to colour in this figure legend, the reader is referred to the web version of this article.)

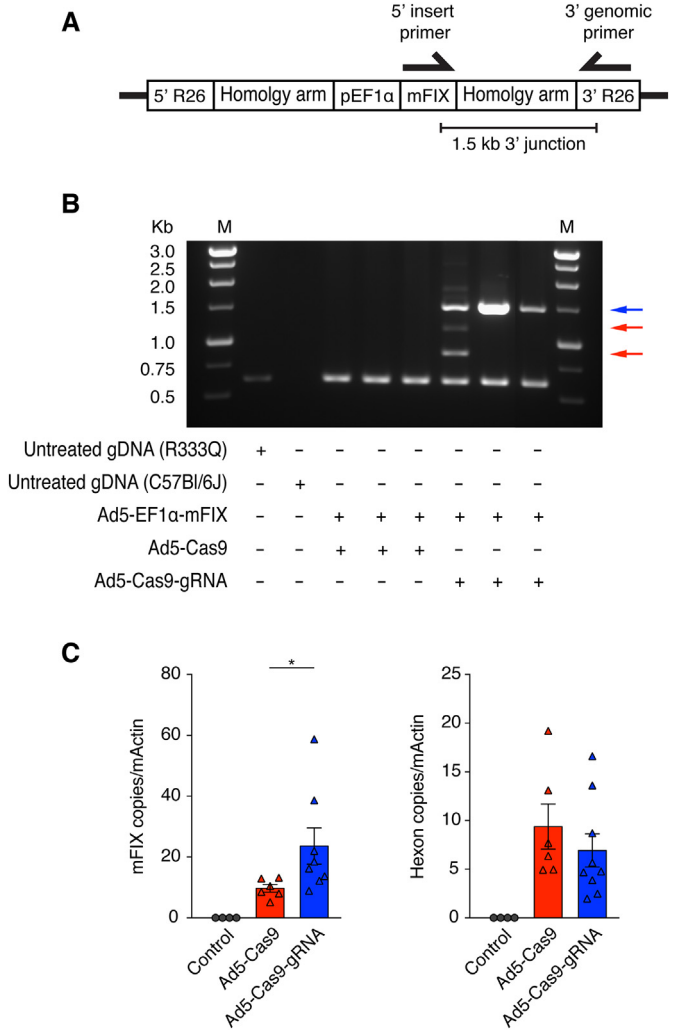

Fig. 4. On-target *mFIX* cDNA integration at *ROSA26*. (A) A schematic showing a *ROSA26* allele containing the integrated *mFIX* expression cassette. Junction capture PCR amplifies the 3′-end of *ROSA26* integrated with the *mFIX* cDNA using a primer set binding in the 3′-end of *mFIX* (black half-arrow, 5′ insert primer) and binding downstream of the target insertion site in the genome (black half-arrow, 3′ genomic primer), past the homology arm. (B) Junction capture PCR reactions were performed using liver extracted genomic DNA from mice at 245 dpi and reactions ran on an agarose gel. *mFIX* cDNA integrated at *ROSA26* was determined by successful amplification of the expected full-length 1.5-kb amplicon (blue arrow), seen in Ad5-Cas9-gRNA treated mice's samples only. Additional amplicons were randomly generated in some animals treated with Ad5-Cas-gRNA, as seen in lane 7, representing on-target but indel-containing insertions (red arrows). Amplicons were gel extracted and Sanger sequenced to confirm identity. Amplification of a 0.62-kb sequence of the adenoviral capsid gene *hexon* was used as a loading control and viral infection control. Each lane represents an individual mouse's DNA as template for PCR. Kb stands for kilo-base and M for marker. Gel is representative of four replicate PCR and gels. (C) Liver DNA extracted at 245 dpi was used to quantify *mFIX* (left) and *hexon* (right) copy numbers normalized to *m-Actin* using qPCR. Each dot represents data from one animal and results are averaged from two independent experiments. Statistics were performed using non-parametric Mann-Whitney *U* tests for non-normally distributed data. p-values are p = 0.0127 for the *mFIX* qPCR and p = 0.2238 for the *hexon* qPCR. (For interpretation of the references to colour in this figure legend, the reader is referred to the web version of this article.)

contrast, plasma from Ad5-Cas9-gRNA treated mice averaged ~5.0%, with a maximum of 10% normal activity.

Secondly, mice were submitted to a tail clip functional assay in which the time for bleeding to stop, due to clotting of the injury, is measured. The clipped tail of wild-type C57Bl/6J control mice bled for approximately 8.0 min, on average, while control untreated R333Q hemophilia mice exhibited protracted bleeding with no signs of diminished blood flow (Fig. 3B). After clippings, all Ad5-Cas9-gRNA treated mice ceased bleeding within the experimental timeframe, averaging 15.5 min of bleeding (Fig. 3B) (plasma mFIX concentration range 241–612 ng/mL). In contrast, mice treated with Ad5-Cas9 bled significantly longer (averaging 25.4 min) with no cessation of bleeding in some mice (Fig. 3B) (plasma mFIX concentration range 25.0–168 ng/mL). The controlled bleeding of Ad5-Cas9-gRNA treated mice represents substantial phenotypic correction of the R333Q strain's

bleeding diathesis, which was not robustly achieved using non-editing Ad5-Cas9. Taken together, results obtained from the ELISA time-course, tail clips, and the enzymatic assay demonstrate that treatment with integration-mediating vectors provides improved phenotypic correction and greater therapeutic value than non-editing vector treatment, in the context of juvenile mice.

2.3. Ad5-Cas9-gRNA treatment results in long-term mFIX cDNA integration at ROSA26, in errorless and error-containing on-target configurations, and increases mFIX copy number

To explore if gene editing occurred in treated mice, and if such editing was still detectable at the end of the time course, liver genomic DNA was used for junction capture PCR. PCR amplicons representing the 3′-junction of *mFIX* cDNA integrated *ROSA26* alleles were detected in the genomes of mice treated with Ad-Cas9-gRNA, but not in any untreated or Ad5-Cas9 treated mice (Fig. 4A and B). In Ad5-Cas9-gRNA treated mice, the presence of a full-sized 1.5 kb amplicon established that homology-directed repair (HDR) of DSBs resulted in on-target integration with Ad5-EF1α-mFIX as the repair template. Sanger sequencing of the amplicon verified correct amplification, genomic origin, and error-free insertion of *mFIX* cDNA at *ROSA26* (Supplemental Fig. 3). Unexpectedly, random amplification of smaller sized alleles were also noted in several mice, albeit less frequently than the full-length amplicon (Fig. 4). Sanger sequencing of these lower MW amplicons from one mouse revealed the presence of on-target but error-containing 'scarred' insertions (Supplemental Fig. 4). Several sizable deletions (109, 209, and 584 bp) were identified at the homology border demonstrating that *mFIX* also integrated through error-prone mechanisms (Supplemental Figs. 5–7). The insertion or deletions (indels) of nucleotides only occurred in regions directly adjacent or part of the homology border region. Interestingly, none of the three identified error-containing alleles had mutations within the coding region of *mFIX*. However, one allele contained a potential 2-bp loss at the end of the poly(A) regulatory sequence (Supplementary Fig. 5). An insertion (+1 bp) at the deletion break point was identified in one allele (Supplemental Fig. 6). In two alleles, deletions occurred with shared bp(s) at the break point (Supplemental Fig. 5 and 7). Overall, these data show that (i) error-free and scarred on-target gene knock-in can occur and (ii) editing of the *ROSA26* locus is still detectable up to 245 dpi. Importantly, the individual mouse with these identified indels at the on-target integration site expressed mFIX throughout the experimental period. The presence of these integrated alleles also demonstrates that gene editing with an adenovirus vector permits large (4.5 kilobase (kb)) cDNA targeted knock-in and persists for a substantial time *in vivo*, likely contributing to long-term gene expression in developing mice.

Next, we used quantitative PCR (qPCR) to determine copy numbers of *mFIX* in uninfected controls, Ad5-Cas9, and Ad5-Cas9-gRNA treated mice (Fig. 4C). We also used qPCR to enumerate remaining viral genomes by measuring the number of *hexon* copies remaining (Fig. 4C). *Hexon* is the primary adenoviral capsid protein gene. In the Ad5-Cas9-gRNA treated group, a significant increase in *mFIX* copies was observed compared to control Ad5-Cas9 treated animals. Of import, no significant differences in remaining viral genome copies were found.

To conduct a preliminary investigation into off-target integration events, we utilized conventional Linear Amplification Method-PCR (LAM-PCR) to generate amplicons of sequences surrounding the *mFIX* transgene. Most captured sequences from two Ad5-Cas9-gRNA treated mice were derived from either the vector genome or potentially from on-target integration (Supplemental Fig. 8). However, we also identified a shared off-target integration site in chromosome 3 (RP24–555P13, Genebank ID AC115945.9) in both examined Ad5-Cas9-gRNA treated mice. No obvious *ROSA26*-gRNA sequence homology was found at the surrounding sequences, with the greatest homology to the *ROSA26*-gRNA target sequence, without bp mismatch, being 10 bp at a 20+ kb distance. Importantly, a *Nhe*I restriction site was identified at the capture sequence validating the integration capture procedure (see Methods). Interestingly, the region in which the integration event occurred is a retrotransposon element (RLTR11A) (chr3:76541–77,051). Additionally, a second off-target integration site was found in one animal occurring at the *Gamma-Secretase-Activating Protein* (*GSAP*) (NM_001359876) locus (Chr5:21186363). Similar to the other identified off-target site, a *Nco*I restriction site was present at the capture sequence and no overt homology to the *ROSA26*-gRNA target sequence was present (see Methods). Alignment of the primer used for generation of linear amplicons did not have homology to sequences at either off-target site, ruling out non-specific primer amplification.

2.4. Therapy with Cas9-expressing vectors elicits anti-Ad5 and anti-Cas9 antibody production

Adenoviral vectors, as well as other viral vectors, have known immunogenicity and recent reports have highlighted potential immunogenicity of Cas9 [32–33]. Due to these reports, we asked if a humoral response could be detected following adenoviral therapy. Plasma taken from mice at 35 and 189 dpi showed an absence of IgG antibodies against mFIX protein, whereas IgG antibodies specifically reactive to the Cas9 endonuclease or to adenoviral particles were detectable at both time points (Supplemental Fig. 9). Plasma from untreated mice showed no reactivity to any of these three components. Thus, the clear presence of anti-Cas9 and anti-Ad5 antibodies shows a humoral response was mounted against this therapeutic approach, following exposure to vector and Cas9 transgene expression.

2.5. Therapy with Cas9-expressing vectors induces Cas9-specific T cell responses and memory T cell formation

Having detected humoral responses to Cas9, we asked whether Cas9 elicits antigen-specific T cell responses in our therapeutic strategy. To do so, we performed *ex vivo* restimulation of splenic T cells from mice treated with adenoviral vectors or naïve controls. At 7 dpi, T cells from Ad5-Cas9-gRNA treated mice produced IFN-γ upon stimulation with antigen presenting cells (APCs) pulsed with recombinant Cas9 (rCas9) or APCs treated with Ad5-Cas9-gRNA but not from untreated controls, indicating that Cas9-specific naïve $CD8^+$ T cell precursors were primed in mice treated with Ad5-Cas9-gRNA (Fig. 5A and C). Additionally, $CD4^+$ T cells also produced IFN-γ in response to rCas9 antigen presentation (Fig. 5B and C). Similarly, Ad5-specific $CD8^+$ T cells from Ad5-Cas9-gRNA and Ad5-mFIX treated mice were detected at 7 dpi, as determined by stimulation with Adpk-GFP treated APCs (Fig. 5A and C) (Supplemental Fig. 10). The use of Adpk-GFP allows increased internalization by APCs compared to standard Ad5 vectors due to enhanced transduction of APCs (Supplemental Fig. 11). Conversely, no mFIX-specific T cells were detected following stimulation with APCs pulsed with recombinant mFIX (rmFIX) (Fig. 5A–C). We also analyzed T cells at 210 dpi and found that Cas9-specific and capsid-specific T cells persisted, albeit at low levels (Supplemental Fig. 12). Boosting of mice with adenoviral vectors at 200 dpi resulted in a small yet detectable memory T cell response. In both contexts, T cells did not expand to levels observed during the acute phase of treatment (Fig. 5). Given that Cas9-specific T cells were still detectable well after initial treatment, we asked if Cas9 may persist *in vivo*. To this end, we successfully PCR-amplified an internal sequence of Cas9 coding sequence (CDS) from liver extracted DNA in treated mice at 245 dpi (Supplemental Fig. 13). The detection of Cas9 DNA at this late time confirms a continued presence of the Cas9 transgene in treated mice. In summary, T cells from treated mice displayed antigen-specific responses to Cas9 and viral particles but not to mFIX. However, total elimination of Cas9 transduced cells did not occur.

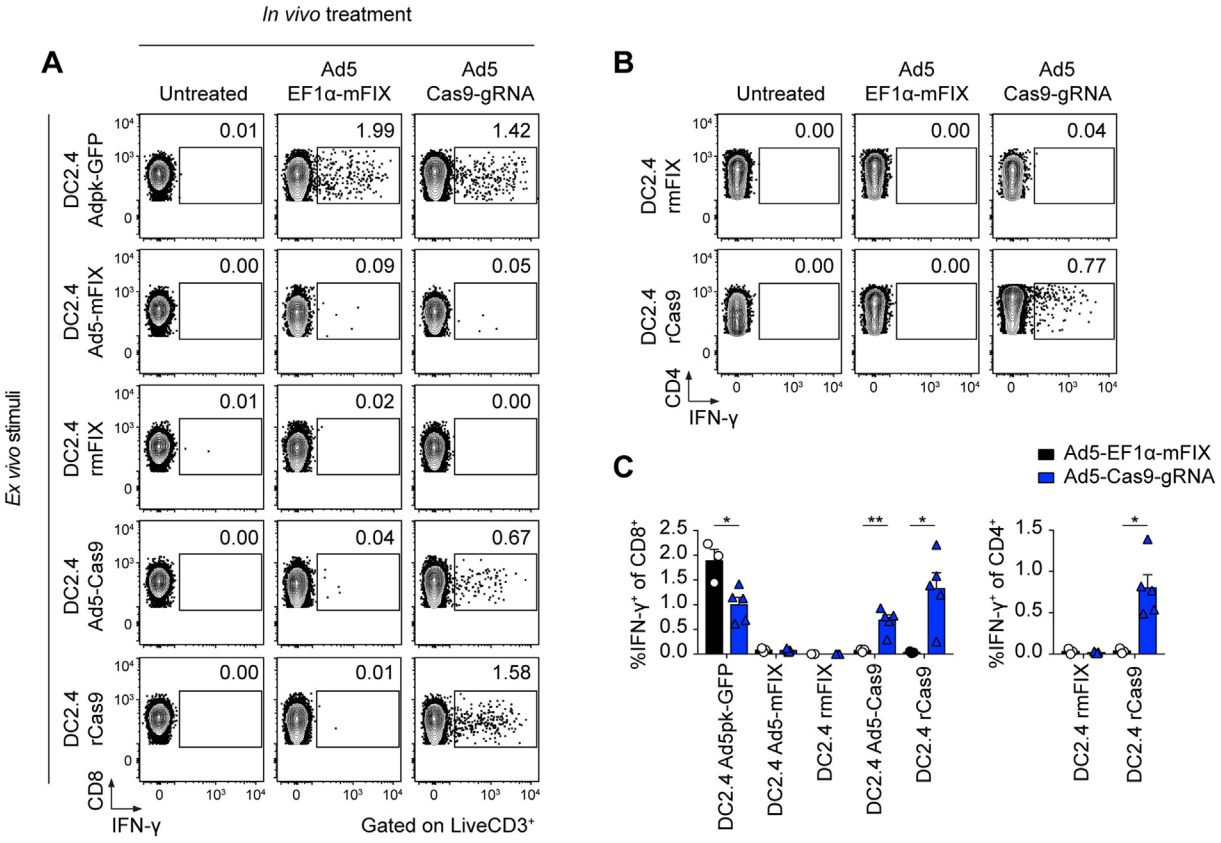

Fig. 5. Antigen-specific T cell responses to adenoviral-mediated gene editing therapy. (A) Mice were injected with PBS (untreated) ($n = 2$), 1×10^{11} viral particles (VP) of Ad5-EF1α-mFIX ($n = 3$) or Ad5-Cas9-gRNA ($n = 5$) (columns). Seven days later, splenocytes were harvested and co-cultured under the indicated stimuli conditions (rows). DC2.4 cells had been cultured prior with stimuli Adpk-GFP, Ad5-mFIX, rmFIX, Ad5-Cas9, or rCas9 allowing internalization, antigen processing and presentation. IFNγ production by T cells was determined by flow cytometry. Representative flow plots of IFNγ production in $CD8^+$ T cells are shown. (B) Splenocytes from untreated or vector-treated mice were stimulated with DC2.4 cells treated with rmFIX or rCas9. Representative plots show IFNγ production in $CD4^+$ T cells, as determined by flow cytometery. (C) Graph showing total quantification of replicate flow data, displaying IFNγ production in T cells ($CD8^+$ T cells in left panel, $CD4^+$ T cells in right panel) based upon DC2.4 antigen stimuli treatment (x-axis) and animal vector injection (colored bars). Statistical analysis was performed by unpaired Student's *t*-test or one-way ANOVA followed by Tukey post-test. Error bars are the SEM. Results are from one animal experiment with two technical replicates. Individual dots represent data from one animal.

2.6. In situ detection of mFIX and vector genomes confirms persistent mFIX expression and residual vector presence

As our gene knock-in strategy yielded long-term therapeutic protein expression despite an immune response, we sought to confirm the presence of mFIX expression and residual vector genomes. In doing so, we also observed differences in *mFIX* transgene and adenoviral genome fates between knock-in (Ad5-Cas9-gRNA) and non-editing (Ad5-Cas9) approaches. Using *in situ* hybridization permitted detection of *mFIX* cDNA and RNA in both *mFIX* knock-in and non-editing treated mice at 245 dpi (Fig. 6A). Additionally, adenoviral genomes were detectable in the nuclei of cells from these mice, independent and co-localized to *mFIX* signal (Fig. 6A). These results support our current and previous findings of continued gene expression and vector persistence [29]. The use of positive control probes displayed signal in nearly all nuclei, while negative control probes showed negligible signal (Supplemental Fig. 14). Probes for *mFIX* showed ubiquitous detection in wild-type C57Bl/6J liver sections and an absence of adenoviral genome detection (Fig. 6A).

Blinded examination of nuclei displaying *mFIX* and/or adenoviral genomic probe signals, from both knock-in and non-editing treated mice (approximately 877 nuclei per mouse), suggested several trends (Fig. 6B). A greater frequency of nuclear *mFIX* transgene or RNA was seen among knock-in treated mice (1469 *mFIX*+ *vs* 1043 *mFIX*+ nuclei). Of note, the incidence of vector genome signal was potentially higher in the nuclei of liver cells extracted from mice treated with non-editing vectors (406 Ad5+ nuclei) compared to mice treated with knock-in vectors (171 Ad5+ nuclei). Additionally, a greater incidence of nuclear co-localization of *mFIX* and vector genomes was seen in non-editing (279 co-localized nuclei) *vs* knock-in treatment (140 co-localized nuclei). These results suggested the possibility that integration-containing mice retained the *mFIX* transgene dissimilarly than non-editing treated mice, witnessed by the observed differences in co-localization, *mFIX* incidence, and vector genome detection.

3. Discussion

Long-term phenotypic correction is a primary objective of inherited disease gene therapy. In general, early generation adenoviral vectors have not been suitable to cure inherited diseases such as plasma deficiencies, due to the transience of therapeutic gene expression [34]. However, several studies have shown this vector can successfully treat inherited disease in select contexts [35–37]. As a proof-of-principle, we demonstrate that adenoviral vectors are capable of corrective gene editing in pediatric inherited disease using a well-characterized disease model, murine HB. In this regard, curative treatments of pediatric HB and other inherited plasma deficiencies must embody methods to overcome issues related to the application of gene therapy in juvenile patients, including vector loss and high cell turnover in developing organs [5]. Although generally considered as a transient vector, adenoviral vectors can persist *in vivo* with low levels of long-term expression [38–39]. The unique ability of adenoviral vectors to persist as

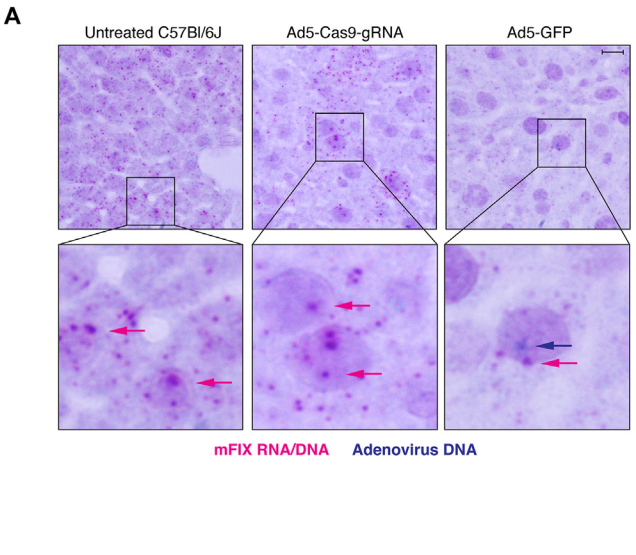

Fig. 6. *In situ* hybridization of *mFIX* RNA/DNA and adenoviral vector genomes. (A) Liver sections from mice treated with 7.5×10^{10} viral particles (VP) of Ad5-EF1α-mFIX and 2.5×10^{10} VP of either Ad5-Cas9-gRNA ($n = 2$) or Ad5-GFP ($n = 2$), as well as untreated C57Bl/6J ($n = 1$), were used for *in situ* hybridization at 245 dpi. Representative images show hybridization of oligo probes targeting *mFIX* RNA/DNA (red dots) and adenoviral DNA (blue dots). Larger images are at 40× zoom, while insets highlight nuclear-localized signals of *mFIX* RNA/DNA (red dots/arrows) and vector genomic DNA (blue dots/arrows) in individual cells. Scale bar is 20 μm. (B) Blinded analysis of 30 random liver section images per group quantified *mFIX* (pink), adenoviral DNA (blue) or co-localized (gray) signals in nuclei. Data is displayed as a percentage of total detected nuclear signals. Percent of detected signals are as follows: C57Bl/6J- 98.5% *mFIX*, 0.3% adenoviral genome, 1.1% co-localized signal; Ad5-Cas9-gRNA treatment- 82.5% *mFIX*, 9.6% adenoviral genome, 7.9% co-localized signal; Ad5-GFP treatment- 60.4% *mFIX*, 23.5% adenoviral genome, 16.1% co-localized signal. Results are from three independent hybridization experiments. (For interpretation of the references to colour in this figure legend, the reader is referred to the web version of this article.)

unintegrated episomes through cellular turnover make it an appropriate tool to compare gene editing versus episomal-based approaches [39–40]. In this study, direct comparison of episomal persistence to a CRISPR/Cas9-mediated knock-in approach revealed that higher levels of stable therapeutic protein expression can be achieved using targeted integration. Importantly, *mFIX* knock-in treated mice expressed > 10% normal FIX levels for nearly the duration of the experiment (averaging 76% at seven dpi to 8.4% normal FIX levels at 238 dpi), well within a 'mild' hemophilia phenotype, representing successful long-term protein expression as the mice matured. Furthermore, the mFIX plasma concentrations of the mFIX knock-in group at 238 dpi (averaging 420 ng/mL) was similar, or greater, than plasma mFIX levels in non-editing treated mice at 35 dpi (averaging 350 ng/mL).

Increased FIX activity in terminal plasma samples from knock-in compared to non-editing treatments supported the findings of the ELISA. The non-editing vector approach provided low residual FIX activity and only minor improvement over untreated mice, representing minimal disease correction. In contrast, integration-based therapy significantly augmented FIX activity in mice, past maturation into adulthood, effectively representing lifelong phenotypic correction [41]. Functional testing of the mice's bleeding diatheses also showed the greatest therapeutic benefit was provided by integration-based treatment. As these three data were in strong agreement, we conclude integration-based treatment conferred an advantage in temporal maintenance of therapeutic protein expression and phenotypic correction following adenoviral-mediated gene transfer in young animals.

As treatment with integration-capable vectors contributed to increased therapeutic efficacy, we sought to verify the presence of edited *ROSA26* alleles. Junction capture PCR confirmed *ROSA26* loci contained errorless HDR-integrated *mFIX* cDNA, present in the livers of treated mice even after 245 dpi. This finding indicated that edited cells persist over a substantial time *in vivo*, editing machinery is active for a continued period, or a combination of both situations occurred. For example, cells edited early may have persisted over time, as hepatocytes are self-renewing, or editing may have occurred in other progenitor cells [42]. Further evidence of edited cell persistence was the observed increase in remaining *mFIX* copies at 245 dpi in Ad5-Cas9-gRNA treated mice. The amount of residual viral genomes remaining in mice at this time point was not significantly different, signifying vector loss was equal between Ad5-Cas9 and Ad5-Cas9-gRNA groups. Thus, the increase *mFIX* copies in Ad5-Cas9-gRNA compared to controls was likely a result of transgene replication following integration in host cells.

Although studies have posited long-term activity of CRISPR/Cas9 is not evident *in vivo*, we detected the *Cas9* gene at late time points, suggesting CRISPR/Cas9 components may persist in animals longer than expected when delivered as a transgene [43–45]. Relevant to this supposition, an *in vitro* study demonstrated prolonged Cas9 activity resulted in unintended editing outcomes [46]. Similarly, in our study, junction capture PCR allowed identification of unexpected *mFIX*-integrated *ROSA26* alleles containing indels at the homology border, resulting from scarred yet on-target cDNA knock-in. These error-containing alleles show additional DNA repair mechanisms may occur with CRISPR/Cas9 use *in vivo*, such as microhomology-mediated homologous recombination and other non-canonical HDR pathways [47]. Another potential explanation is an initial DSB was repaired by non-homologous end joining (NHEJ) causing indels within sequences surrounding the gRNA target site, but also correctly repaired the gRNA recognition sequence. A second DSB could then be repaired *via* HDR, resulting the scarred insertion. To our knowledge, this is the first report of on-target insertions containing indels *in vivo* when using viral delivery of CRISPR/Cas9 as a therapy. To reduce the chance for errors affecting the coding sequences of a therapeutic gene cassette, future HDR-based approaches may seek to include large homology arms or insulating sequences in the border regions of repair templates. Indeed, increasing evidence of large deletions and complex genomic rearrangements continues to be reported [48–49]. However, such findings are derived from *in vitro* and zygotic injection experiments, both highly proliferative contexts whereby DNA repair pathway activities likely differ compared to *in vivo* somatic gene editing.

Although we focused on characterizing on-target integrations, we did perform a preliminary examination of off-target integrations. By capturing sequences surrounding the *mFIX* expression cassette at 245 dpi in the livers of two mice, we surprisingly identified two off-target integration sites (Supplemental Fig. 8). Interestingly, the off-target integration junctions appear to have occurred near the poly(A) regulatory element and surrounding residual sequences from the cloning vector, which may also impact future knock-in repair template designs. However, the limitations of our LAM-PCR protocol use (*i.e.* clonal analysis) is not a strictly quantitative method as it is dependent on two nested PCRs, size-based ligation efficiencies, and the presence of restriction sites near integration sites. Of note, the *ROSA26* target locus does not have a nearby restriction enzyme site of the four enzymes we used. Thus, the frequency of on-target *versus* off-target integration using

Ad5-mediated delivery *in vivo* is not yet determined. As we were unable to find any evidence of homology to the gRNA target sequence at off-target integration regions, the relationship between the use of CRISPR/Cas9 editing and the off-target integration events is unclear. Importantly, prior research using this *ROSA26*-targeting gRNA found minimal off-target editing at top computationally-predicted sites and the total identification of off-target effects is beyond the scope of this proof of principle study [29]. Altogether, our examination of on- and off-target integration sites have direct implications for gene editing approaches that seek to use CRISPR/Cas9 for insertion, especially approaches targeting correction of small mutations or endogenous disease loci.

Adenovirus is not considered to randomly integrate into host chromosomes at an appreciable rate, however this topic has not been re-examined recently and could explain observations of prolonged persistence of vector genomes [28]. Although studies have observed random adenoviral genome integration, the majority of adenoviral persistence is believed to be a result of episome maintenance [40]. Thus, the residual persistent gene expression seen in our control groups is likely the result of long-term maintenance of episomal viral genomes, but we cannot currently exclude out the possibility of random viral integration. Additionally, adenoviral episomes have a characterized ability to persist through cell divisions, unlike other vectors such as rAAV, a characteristic which may explain our prolonged detection of adenoviral genomes and gene expression following application in young animals [39–40].

Although persistent protein expression was observable in all treated mice, albeit at different levels, a common gradual reduction in expression suggested that certain mechanisms reduced expression. The cause of expression loss following adenoviral-mediated gene transfer is an area of intense study [39,50]. Several reports have highlighted the impact of epigenetic silencing, immunological clearance, and cell turnover on the loss of gene expression [50–53]. Knowing adenovirus can elicit diverse immune responses, we focused on adaptive immune responses to three components of our therapy: adenoviral particles, Cas9 nuclease, and mFIX. We determined treated mice developed humoral immunity against both Cas9 and the viral particles by 35 dpi, persisting to at least 189 dpi (Supplemental Fig. 12). Although antibody formation against adenoviral particles is well characterized, the formation of anti-Cas9 IgG following a gene therapy has been described infrequently in the context of the CRISPR/Cas9 system's extensive use [30]. Additionally, recent publications have highlighted the presence of anti-Cas9 antibodies in normal human populations, an important consideration for clinical implementation of CRISPR/Cas9 [54–55]. Considering these findings, we assayed for antibody formation against the mFIX protein, a major issue in hemophilia treatment, but did not detect IgG-reactive to mFIX. The R333Q strain's circulating non-functional human FIX (hFIX) may have permitted avoidance of a humoral response against mFIX, due to self-tolerance of hFIX. These findings do not exclude other potential classes of immunoglobulins which may have developed.

After identifying humoral responses against our therapy, we explored whether other adaptive immune responses occurred by measuring antigen-specific T cell responses. As early as 7 dpi with adenoviral vectors expressing CRISPR/Cas9 components, a significant percentage of $CD8^+$ and $CD4^+$ T cells were specifically reactive to Cas9 and the viral particles. T cell-mediated IFNγ production from recognition of cognate capsid and Cas9 antigen was also detectable as late as 210 dpi, suggesting that adenoviral-mediated gene editing results in the formation of memory T cells; this finding has direct implications for repeat application of CRISPR/Cas9 therapies or use in people with preexisting anti-Cas9 immunity. As both Cas9-specific $CD8^+$ and $CD4^+$ T cells were primed following adenoviral therapy, the antigen was processed and presented *via* the major histocompatibility complex (MHC) class I and MHC class II pathways in treated mice. However, the relevant APC and mechanisms of T cell priming is yet undetermined.

Our demonstration of T cell-mediated IFNγ production in response to Cas9 supports other recent studies finding immunological consequences of CRISPR/Cas9 systems [32–32,54–57]. Similar results have been found using human samples, however we identified antigen-specific T cell subsets, following a CRISPR/Cas9-based therapy. Taken together, we postulate these adaptive responses directly influenced the observed protein expression profiles in our study. We also assume that the induction of partial tolerance was possible, as the *Cas9* gene persisted and knock-in alleles were still detectable; therefore, all transduced and edited cells were not eliminated. This theory is supported by the findings that recombinant adenoviral vectors can induce an exhausted T cell phenotype *in vivo* [58]. Furthermore, a balance of anti-Cas9 effector and regulatory T cells has been described in humans [59]. This recent publication illustrating Cas9 reactive T cells in humans has direct relevance to our findings of $CD8^+$ and $CD4^+$ reactivity following a therapeutic approach; together they imply that direct CRISPR/Cas9 use in humans will require strategies to mitigate immune activation (*e.g.* immunosuppressive corticosteroids), strategies to induce tolerance to Cas9 prior to treatment, or depletion of Cas9-reactive immune cells. In our study, the 'boosting' of mice with additional vector did not appear to increase the magnitude of reactive T cells, and, importantly, did not cause any lethality. Indeed, no mortality or overt signs of oncogenesis was associated with the therapy in this study, consistent with our prior findings [29]. The failure of 'boost' injections to recall memory T cells was perhaps due anti-Ad5 antibodies, which can limit transduction efficacy [60]. However, we do not exclude the possibility that other cells involved in innate immune responses, such as macrophage and NK cells, influenced mFIX expression [61]. In total, we posit Cas9 is a challenge to clinical applications, due to its immunogenicity derived from natural exposure and following a therapy [32]. Furthermore, we provide initial evidence that the Cas9 gene can persist *in vivo*, a potential risk that must be fully elucidated by future studies. Thus, future studies should explore methods to limit immune responses to vector and gene editing components, determine vector influence, and means to control spatial and temporal Cas9 activity.

Knowing vector treatment evoked cellular and humoral responses, likely coinciding with inflammation and transient liver toxicity as reported previously, we explored a potential means by which edited alleles persisted [53,61]. As mice were injected prior to maturation and adenoviral vectors can induce substantial cell cycling due to liver regeneration following vector-mediated toxicity, akin to partial hepatectomies, we theorize appreciable cell cycling may have occurred post-therapy [62]. The use of RNAscope technology allowed *in situ* observation of nuclear signals of *mFIX* DNA and RNA, as well as adenoviral episomes. The observations pointed towards a higher frequency of *mFIX* nuclear signals and less co-localization to vector genomes in integration-mediating vector-treated mice consistent with our qPCR data. In the context of a developing and regenerating liver, any cell that underwent a *mFIX* integration event would replicate the integrated transgene at every cell division. Such cellular turnover could theoretically support long-term maintenance of *mFIX* alleles and higher stable protein expression, while avoiding silencing mechanisms which can affect episomal-based expression. This mechanism could also lead to a dilution of vector genomes, as seen in our nuclear signal observations and proposed in other reports [33]. In this study, we qualitatively show knock-in *versus* non-editing treatment may result in differences of nuclear co-localization and transgene retention, an observation not inconsistent with the above supposition.

Overall, we demonstrated adenoviral vectors are a suitable platform for gene insertion in the context of diseased non-adult animals. By treating in the adolescent stage, the risk of germline transmission of transgene and vector sequences is reduced compared to prenatal and intrauterine gene editing [19,63]. In this context, the early generation Ad5-based vector used in this study would not likely be an optimal choice for clinical application due to pre-formed immunity and its known immunogenicity in humans. However, alternative non-human or

rare serotype with reduced immune reactivity in humans may be suitable candidates for future gene editing approaches. Notably, adenoviral vectors can be rationally targeted; cell-specific delivery of gene editing systems could be useful for diseases which arise from distinctive cell types. Moreover, adenoviral vectors may be applicable to other diseases requiring large cloning capacity, such as von Willebrand disease or hemophilia A using helper-dependent vectors devoid of viral genes [25–26].

This study provides a critical proof-of-principle that a universal gene editing platform is feasible for treating plasma deficiencies. Importantly, complete cDNA knock-in at a safe harbor is potentially applicable to all patients, regardless of causative mutations. Of note, our correction of HB using gene knock-in is contrary to another study reporting that adenoviral vectors are unsuitable for gene editing, due to toxicity [64]. Our approach benefited from episomal expression augmenting cDNA knock-in targeting a safe harbor locus. We do not target the endogenous FIX locus, a context whereby NHEJ and other error-prone DNA repair mechanisms induce new potentially deleterious mutations [45]. Thus, we believe universal cDNA integration at a safe harbor strategy has several advantages compared to correction of the endogenous disease-causing gene. Targeting a single locus may yield more consistent results and off-target effects than targeting numerous causative mutations with varying sequence composition and locus position. Thus, avoiding of the introduction of new mutations at the disease locus (occurring through NHEJ activity), applicability to numerous diseases (rather than a disease-specific therapy tailored per mutation), and production feasibility make safe harbor targeting a compelling strategy. However, exceptions to this approach are diseases requiring endogenous gene regulation (*e.g.* expressing the gene at specific times during developmental processes) and diseases with dominant negative mutations.

The increase in therapeutic efficacy was modest in this study, enough to have value in the context of hemophilia treatment. Comparison of plasma levels achieved in this study to normal murine levels (normal murine FIX plasma level is 2.5 μg/mL) might suggest greater correction [65]. Additionally, the hemostatic effect of our approach may be greater in FIX null mice, due to a likely antagonism between the dysfunctional hFIX in the R333Q strain and the provided therapeutic mFIX. In the future, optimized expression cassettes, stronger promoters, long-lasting, and hyper-functional proteins can be applied to increase efficacy [66–67]. Improvements in HDR efficiencies and optimized editing approaches, such as multiplexed targeted integrations, could also lead to higher levels of therapeutic protein. Future studies should also assess the risk of germline transmission to address if vectors reach gametocytes and other critical preclinical studies to determine vector shedding, further examination of vector persistence, and the possibility of vector reactivation. Overall, we demonstrate that somatic gene editing for pediatric plasma deficiencies can be standardized and is feasible with viral vectors.

4. Conclusions

In summary, this proof-of-principle study shows a universal knock-in approach can provide significant improvements over non-editing vector treatment by providing robust long-term phenotypic correction. Notably, the use of adenoviral vectors may find applications to treat diseases that other vectors cannot, such as those constrained by packaging capacity. We find gene editing *in vivo* comprises on-target knock-in through HDR but also from error-containing insertions, and knock-in editing outcomes persists for a substantial time. Long-term phenotypic correction was achieved using our straightforward approach, despite elicitation of B and T cell immune responses, supporting the further development of editing-based strategies for treatment of pediatric inherited plasma deficiencies. We highlight that therapeutics involving CRISPR/Cas9 are certainly viable, but preclinical studies should recognize and address potential immune and genetic consequences that may occur post-treatment.

5. Methods

5.1. AdV5 vector constructions

The adenoviral vectors Ad5-Cas9-gRNA, Ad5-Cas9, and Ad5-gRNA were constructed as described previously (Fig. 1) [29]. A HDR template vector, was generated expressing mouse FIX (*mFIX*) cDNA. First, *mFIX* was digested from plasmid pGem-mFIX (Sinobiologicals, Beijing, China) using *Zra*I and *Eco*53kI. The pBapoEF1α plasmid (Clontech Laboratories, Mountain View, CA) was digested with BamHI and *Hin*dIII, then Klenow-fragment and calf-alkaline phosphatase treated. The *mFIX* cDNA was sub-cloned into pBapoEF1α for expression control by the human EF1α promoter and HSV-TK polyadenylation transcription terminator. Sequencing confirmed correct orientation, resulting plasmid pBapoEF1α-mFIX. The expression cassette was restricted using *Cla*I, Klenow-fragment treated, and ligated into the *Pme*I site of a *ROSA26* HDR repair template plasmid, provided by the Genome Engineering and iPSC Center at Washington University School of Medicine (WUSM). This plasmid, pROSA26, contains ~800 bp of sequences homologous to the *ROSA26* locus, flanking the gRNA target site [29]. In this targeting repair template, the *ROSA26* gRNA does not cut the template as the gRNA target sequence is mutated by the insertion of a multiple-cloning site, effectively abolishing gRNA recognition. pROSA26-EF1α-mFIX digestion with *Pvu*II generated a fragment containing homology sequences and the *mFIX* expression cassette for ligation into the *Eco*RV site of pShuttle (Agilent Technologies, Santa Clara, CA), an adenoviral E1-region shuttle plasmid (lacking any promoter), making pShuttle-EF1α-mFIX-ROSA26. Following linearization with PmeI, this shuttle plasmid was recombined into the E1-deleted region of pAdEasy-1 plasmid (human adenovirus C serotype 5 [Ad5] genomic plasmid) (Agilent Technologies) in *Escherichia coli* (*E. coli*) BJ5183, to generate pAd-EF1α-mFIX (Fig. 1). All restriction enzymes and nucleases were purchased from New England Biolabs (Ipswich, MA).

Additional control vectors were constructed similarly but lack any *ROSA26* homology sequences or CRISPR/Cas9 genes (Supplemental Fig. 10). Briefly, the *mFIX* cDNA fragment was inserted into pShuttle-CMV (Agilent Technologies) at the EcoRV site, under control of the CMV promoter, and recombined into pAdEasy-1, generating pAd-CMV-mFIX. Additionally, previously described Adpk-EGFP, which contains a modified capsid generated by replacement of the Ad5 fiber knob with porcine adenovirus-4 fiber knob resulting in increased DC2.4 transduction, and Ad5-EGFP were also used (Supplemental Fig. 11) [68–69].

5.2. Tissue culture

Human embryonic kidney 293 (HEK-293) cells (Microbix Biosystems Inc. Mississauga, Ontario, Canada), BNL 1NG A.2 (ATCC, Manassas, VA), and A549 cells (ATCC) were cultured in DMEM-F12 Mix (Lonza-BioWhittaker, Basel, Switzerland) with 10% or 2% FBS (Sigma-Aldrich, St. Louis, MO). The dendritic cell line DC2.4 cells were a kind gift from Dr. Kenneth Rock (University of Massachusetts Medical School) and primary splenocytes were incubated in RPMI media (Sigma-Aldrich) supplemented with 10% FBS. Cell culture was performed in sterile conditions and cells incubated at 37 °C in an atmosphere of 5.0% CO_2.

6. Adenovirus production

Viral generation was performed using standard techniques [70]. Briefly, adenoviral genome-containing plasmids were digested with *Pac*I releasing the recombinant viral genomes, for transfection into HEK-293 cells. After rescue and serial amplification, viruses were purified through ultra-centrifugation in cesium chloride gradients. Partial sequencing of purified virus genomes confirmed vector constructs.

Expression of vector-encoded transgenes was confirmed *via* Western blot (data not shown). Titrations on replication-restricted A549 cells verified absence of replication-competent adenoviral (RCA) contamination. Gene editing knock-in with Ad5-Cas9-gRNA and isogenic donor vectors, encoding other transgenes in the exact configuration of Ad5-EF1α-mFIX, have been reported [29].

6.1. In vitro Indel formation assay

The immortalized murine BNL-1NG A.2 cell line was seeded at 5×10^5 cells per well on six well plates and grown to confluency. One well per plate was harvested and cells counted. Next, PBS, 2×10^3 VP, 4×10^3 VP, 8×10^3 VP, or 12×10^3 VP of Ad5-Cas9-gRNA or Ad5-Cas9 were added to individual wells. 96 h later, cells were harvested and submitted for Illumina targeted deep sequencing of the *ROSA26* locus. The results are from two independent experiments.

6.2. Animal studies

A murine model of HB, referred to as R333Q strain, was maintained as a homozygous inbred colony. This strain was previously generated by the knock-in of defective *hFIX* cDNA (containing an R to Q missense mutation at the FIX catalytic domain effecting FIXa/FVIIIa binding) into the endogenous *mFIX* locus in a C57Bl/6J background [71]. Thus, R333Q mice express a missense non-functional hFIX variant (less than < 1% FIX activity) and no mFIX. This model recapitulates most human HB cases whereby circulating FIX is present (~70% of cases) yet has reduced or absent function. R333Q genotype was confirmed using primers (Table 2) (Primers 1–2) for the neomycin (*neo*) gene residing within the *hFIX* insertion cassette. Further genotyping ensured the absence of wild-type murine *FIX* with a forward primer (Primer 3) located in intron 1 region and a reverse primer in intron 2 of *Mfix* (Primer 4) (Supplemental Fig. 15). C57Bl/6J mice (Jackson Laboratory, Bar Harbor, ME) served as wild-type controls. Male and female mice were used in all groups throughout the study. In humans, HB is X-linked and mostly affects males. However, the use of a single sex in animal studies can introduce sex-based bias, including gene therapy studies [72]. Inclusion of both genders potentially diminishes such bias and allows extrapolation of results to other plasma deficiencies affecting both males and females.

Four weeks old R333Q hemophilia mice were tail vein injected with 7.5×10^{10} viral particles (VP) Ad5-EF1α-mFIX and 2.5×10^{10} VP of either Ad5-Cas9-gRNA ($n = 9$) or Ad5-Cas9 ($n = 7$) in PBS solution. Blood was collected approximately biweekly from the submandibular vein into heparin-coated capillaries (Thermo Fisher Scientific, Waltham, MA) for ELISA quantification of mFIX. Heparinized blood was centrifuged, plasma aliquoted, and stored at −80 °C until use. Prior to injection, a limit of at least 20% normal FIX level at the initial time point was set as a requirement for inclusion in the temporal gene expression experiment, along with optimal injection noted at time of viral administration. Plasmas for mFIX enzymatic assays were collected into an approximate 1:9 volume ratio of 3.8% sodium citrate (Sigma-Aldrich) to blood. Citrated blood was collected from the tail vein during the tail clip assay (245 dpi) and separately from submandibular vein (238 dpi), a week prior to tail clip.

6.3. mFIX ELISA

An optimized sandwich ELISA was developed using affinity-purified anti-mFIX polyclonal antibodies (Cat. # 442404, Lot 1,194,200) (Sinobiologicals). MaxiSorp polystyrene 96-well plates (Thermo Fisher Scientific) were coated with 2.0 μg/mL primary capture antibodies in sodium carbonate buffer [pH 8.5] (Corning Inc., Corning, NY) and stored at 4 °C. Plates were blocked with 2.5% BSA (Santa Cruz Biotechnology, Dallas, TX) in PBS and 0.05% Tween 20 (Sigma-Aldrich). Washes were performed with 0.05% Tween 20 in PBS. All samples, detection antibodies, and standards were diluted in HiSpec Diluent (Bio-Rad Laboratories, Hercules, CA) spiked with pooled mFIX-deficient plasma from untreated R333Q hemophilia mice. Secondary antibody was generated by HRP-conjugation (SeraCare, Milford, MA) of the capture antibody and used for detection at 2.5 μg/mL. Chromogenic development using 3,3′,5,5'-Tetramethylbenzidine (TMB) (Sigma-Aldrich) followed by acidic stop solution (Invitrogen, Carlsbad, CA) allowed reading of OD values at 450 nm.

Serially diluted recombinant mFIX (Sinobiologicals), ranging 62.5 ng/mL to 3.906 ng/mL, was used on each plate to generate a

Table 2
A list of oligonucleotide primer sequences and their corresponding application in this study is provided.

Primer details		
Primer number	Sequence	Use
1	FWD-5′- TGCTCCTGCCGAGAAAGTATCCATCATGGC-3′	R333Q Genotyping
2	REV-5′-CGCCAAGCTCTTCAGCAATATCACGGGTAG-3′	R333Q Genotyping
3	FWD-5′-CAAGAGATGACAAAGTGGGAACTTAACTGC-3′	Wild-Type Genotyping
4	REV-5′-TATGGAGTCACCTCTCTAGTTCCACACTCC-3′	Wild-Type Genotyping
5	FWD-5′-CCGTGAAGGAGGCAAAGATTCG-3′	*mFIX* Junction Capture PCR
6	REV- 5′-AAGCTCACAAGACCTTAGGTCAGGAAAGAC-3′	*mFIX* Junction Capture PCR
7	FWD 5′- CGTACGAGGAGGCACTAAAGC-3′	*Hexon* Amplification
8	REV 5′-ATCCTCACGGTCCACAGGG-3′	*Hexon* Amplification
9	FWD-5′-[Btn]GTCCTGTGAACCAACAGTTCC-3′	LAM-PCR ssDNA Amplification
10	5′-CTAGCGTGGTGAACTGGAACACCTCCTACGAGC[3d_C]-3′	LAM-PCR Linker
11	5-CTGAAGGCTCAGGTTACACAGGCACGCTCGTAGGAGGTGTTCCAGTTCACCACG-3′	LAM-PCR Linker
12	FWD-5′-CCGTGAAGGAGGCAAAGATTCG-3′	First Nested PCR
13	REV-5′-CTGAAGGCTCAGGTTACACAGGCAC-3′	First Nested PCR
14	FWD-5′-GTGTTGGGTCGTTTGTTCATAAACGC-3′	Second Nested PCR
15	REV-5′-GCTCGTAGGAGGTGTTCCAGTTCACC-3′	Second Nested PCR
16	FWD-5′-GCGAGAACCAGACCACCC-3′	Cas9 CDS Amplification
17	REV-5′-CGAGTTATTAGGCGTAGTCGGGCA-3′	Cas9 CDS Amplification

standard curve for calculation of sample mFIX concentrations (Supplemental Fig. 16). mFIX concentrations in plasma samples were calculated from OD values within the linear range of the standard curve and at least twice the standard deviation of the zero value. Cross-reactivity to hFIX was minimal and only detectable at very low sample dilutions using this ELISA system. To control for detection due to the minor cross-reactivity, plasma from untreated R333Q mice was diluted at the same ratio as treated samples. These control dilutions were used to calculate if background was detected from cross-reactivity to the circulating non-functional hFIX (of the R333Q strain) on each plate. Any detection from control animals' plasma background was subtracted from sample values at the corresponding dilution. *Bona fide* detection of mFIX was confirmed by measuring OD 450 nm values of plasma dilutions seven days prior and seven dpi with Ad5-EF1α-mFIX (Supplemental Fig. 1). All plasma samples were run at multiple dilutions in duplicate and time points repeated. Total ELISA results are from two independent animal experiments.

6.4. mFIX enzymatic activity assay

An enzymatic assay (Aniara Diagnostica, West Chester, Ohio) was used to measure mFIX activity in plasma of treated and un-treated mice. The assay consists of a purified protein cascade with a chromogenic readout. Briefly, purified phospholipids, calcium and activated FXI are provided to activate mFIX within the plasma samples, generating mFIXa. Then, the supplied thrombin-activated FVIII (FVIIIa) enzymatically complexes with FIXa activating FX. FXa hydrolyzes the chromogenic substrate, freeing paranitroaniline (pNA). The amount of pNA released is measured by absorbance at 405 nm and is directly proportional to the concentration of FIX in the sample. A standard curve was generated using serially diluted pooled plasma from C57Bl/6J mice diluted into pooled mFIX deficient plasma (R333Q sourced). The assay procedure was performed according to manufacturer's instructions. Negative controls consisted of untreated R333Q animals ($n = 11$), while positive controls consisted of untreated C57Bl/6J mice ($n = 10$). All samples were diluted into diluent spiked with pooled mFIX-deficient plasma. Samples were tested at dilutions from 1:5 to 1:20, with all samples being tested at one dilution per test. Standard curve ranged from 0.5% to 20% normal mFIX activity. Plasma from the submandibular vein and tail vein were analyzed separately and FIX activities measured in each mouse averaged. Results shown are from three independent tests.

6.5. Tail clip assay for functional correction

To assay animals' ability to control bleeding following an injury, a terminal tail clip approach was used. 245 days after injection, treated and untreated mice's tails were clipped at a diameter of 2.0 mm. The clipped tail was intermittently dabbed onto filter paper and the time until bleeding stopped was measured. The bleeding assay was terminated at 30 min to limit animal suffering and participation time. Positive controls consisted of wild-type C57Bl/6J mice ($n = 9$), while untreated R333Q hemophilia B mice ($n = 9$) were used as negative controls.

6.6. Junction capture PCR of mFIX-integrated ROSA26 alleles

DNA extraction from homogenized liver tissue was performed by incubation at 55 °C for several hours in the presence of 1.0% SDS (Sigma-Aldrich), RNaseA (GE Healthcare, Chicago, IL) and proteinase K (Thermo Fisher Scientific). DNA was purified through phenol/chloroform extraction and precipitation with 100% ethanol (Thermo Fisher Scientific) and 3 M sodium acetate [pH 5.2] (Thermo Fisher Scientific). DNA concentration was calculated using an absorbance value of 1.0 at 260 nm being equivalent to 50 μg/mL of DNA and the quality of DNA checked on agarose gel.

To validate gene editing and targeted integration, amplification of the 3′-end of *ROSA26* alleles containing integrated-*mFIX* was performed using liver extracted DNA. One primer binding within *mFIX* cDNA (Primer 5) and a second primer (Primer 6) binding in the genomic region of *ROSA26* (past the homology border) amplified the integration junction. PCR reactions consisted of 5× PhireII buffer, dNTPs (Thermo Fisher Scientific), primers (5 μM), 350 ng of DNA template, and 0.5 μL of PhireII polymerase (Thermo Fisher Scientific). Primers were annealed at 69 °C and amplicons visualized on agarose gels by ethidium bromide staining. Results shown are representative of four independent PCRs. Amplicons were gel-extracted and Sanger sequenced, confirming genomic origin and targeted integration. Loading control consisted of amplification of a 619-bp fragment of the adenoviral gene *hexon* using two primers (Primers 7–8).

6.7. Quantification of mFIX and hexon copies using qPCR

qPCR reactions and cycling were performed as described in detail elsewhere [29]. Briefly, a standard curve for *m-Actin* was generated using serial dilutions of optically pure genomic DNA from an untreated C57Bl/6J mouse and the assumption that one copy of *m-actin* is present in the mouse genome of 2.8×10^9 bps. The second standard curve was generated using serial dilutions of the vector plasmid pAd5-EF1α-mFIX, which contains one copy of *mFIX* cDNA and *hexon*. A commercial primer pair and hydrolysis probe (conjugated to 6-carboxyfluorescein [6-FAM]) specific for *mFIX* (spanning an exon/exon junction) (mm01302526_m1, Thermo Fisher Scientific) or a primer/probe for *hexon,* described elsewhere, were used in separate reactions to quantify copy numbers of each. In each reaction a separate [VIC]-conjugated probe and primer pair specific for *m-actin* DNA (mm00607939, Thermo Fisher Scientific) was included to normalize copy numbers. Each mouse sample was run in duplicate and the results shown are averaged from two independent qPCRs.

6.8. LAM-PCR to capture off-target integrations

LAM-PCR was performed essentially as described in detail elsewhere [17,73]. In brief, a biotinylated primer (Primer 9) spanning an exon/exon junction (to avoid priming to the portions of endogenous *mFIX* gene intact in the R333Q model) and specific to *mFIX* cDNA was used to generate linear ssDNA amplicons of surrounding sequences from whole liver DNA of two mice injected with 7.5×10^{10} VP of Ad5-EF1α-mFIX. Following second strand synthesis, amplicons were digested with *Nhe*I, *Avr*II, *Xba*I, and *Nco*I and ligated to linkers with corresponding sticky ends. Linkers were produced as described elsewhere, with the NcoI linker being described previously [17,29,73]. However, the novel linker compatible to NheI, AvrII, and XbaI overhangs sequences are provided (Primers 10–11). Using the known sequences of the ligated linker, two nested PCRs were performed (Primers 12–13, Primers 14–15). PCR amplicons were then purified, blunt end cloned into the pCR-XL-2-TOPO plasmid (Thermo Fisher Scientific) and transformed into OmniMAX-2-T1^R *E. coli* (Thermo Fisher Scientific). 14 clones were analyzed by Sanger sequencing and BLAST aligned to determine sequences surrounding the *mFIX* cDNA [74]. Results are from one LAM-PCR preparation and six independent nested PCR preparations.

6.9. PCR amplification of the Cas9 gene

A 2.0-kb internal sequence of *Cas9* was PCR-amplified from liver extracted DNA using two primers (primers 16–17). Results shown are representative from two independent PCRs. Positive controls consisted of the pAd-Cas9-gRNA plasmid, used for viral generation, and liver extracted DNA taken 3 dpi with 1×10^{11} VP of Ad5-Cas9-gRNA. Negative controls consisted of the unmodified parental pAd-Easy1 plasmid and liver DNA of an untreated R333Q mouse. Loading controls

consisted of amplification of a 619-bp fragment of *hexon*.

6.10. Assay for antibody formation against adenovirus, Cas9, or mFIX

Recombinant mFIX (Sinobiologicals), recombinant *sp*Cas9 (rCas9) (PNA Bio Inc., Thousand Oaks, CA), or empty adenovirus particles were immobilized on MaxiSorp 96-well plates at 50 ng/well in carbonate coating buffer overnight at 4 °C. Adenoviral particle mass was estimated using the MW of an adenoviral particle as 150×10^6 Da [75]. Plates were blocked with PBS containing 2.5% BSA and 0.5% Tween 20. Plasma samples were sourced from untreated mice ($n = 3$), mice treated with Ad5-EF1α-mFIX and either Ad5-Cas9 ($n = 4$ for rCas9 and capsid, $n = 5$ for rmFIX) or Ad5-Cas9-gRNA ($n = 4$ for rCas9 and Ad5 capsid, $n = 6$ for rmFIX). Plasma was obtained from mice at 35 and 189 dpi and diluted into HiSpec Diluent spiked with pooled untreated R333Q plasma. Plasma dilutions were incubated in duplicate on the protein coated plate. Wells were washed and 0.5 μg/mL of polyclonal goat anti-mouse-IgGs HRP-conjugated antibody (Cat# P0447, Agilent Technologies) was applied to detect the presence of plasma IgG antibodies specifically reactive to proteins coating the wells. Detection of the secondary antibody was performed using TMB for OD measurements at 450 nm. Positive control for viral particle coating and detection was a murine antibody raised against adenoviral capsid fiber protein (clone 4D2, Thermo Fisher Scientific). Positive control for rCas9 coating was a polyclonal rabbit anti-Cas9 antibody (Cat# 632607, Takara Bio Inc., Shiga, Japan) detected with HRP-conjugated goat anti-rabbit IgG (Cat# P0448, Agilent Technologies). Recombinant mFIX coating was positively confirmed using direct detection with an HRP-conjugated anti-mFIX antibody (Cat# 79804, GeneTex Inc., Irvine, CA). Additional assay functionality was validated by the immobilization of His-tagged alpha1-antitrypsin protein (Sinobiologicals), followed by recognition with monoclonal anti-His-tag murine IgG (Cat# 34670, Qaigen, Hilden, Germany) and detection by the same goat anti-mouse IgG-HRP antibody used for the plasma sample IgG detection. Negative controls consisted of untreated mouse plasma, wells incubated without secondary detection antibody, and wells without plasma incubation. Results are from two independent test with all samples in duplicate.

6.11. Stimulation assays for antigen-specific T cell responses

Antigen-specific T cell responses were assayed by *ex vivo* restimulation as previously described [76]. Seven days prior to the assay, 10 weeks old R333Q hemophilia B mice were injected with either PBS (naive control, $n = 2$), 1×10^{11} VP of Ad5-Cas9-gRNA ($n = 5$) or Ad5-EF1α-mFIX ($n = 3$). Three dpi, two replicate 96-well plates (Techno Plastic Products AG, Trasadingen, Switzerland) were seeded with 9×10^4 DC2.4 cells per well. The next day DC2.4 cells were transduced with 2000 VP/cell of either: Adpk-GFP (an Ad5 vector with the knob portion of the fiber capsid protein replaced with porcine adenovirus 4 fiber knob permitting strong DC2.4 transduction), Ad5-mFIX, or Ad5-Cas9 (Supplemental Figs. 10–11) [68]. Separately, DC2.4 cells were fed 10 μg/mL rCas9 or 7 μg/mL rmFIX. Seven dpi mice were sacrificed, spleens harvested, and cells ground through a 70-μm cell strainer. RBCs were lysed and 1×10^6 splenocytes plated into wells containing the DCs of above stimuli treatments. Splenocytes and treated DC2.4 cells were co-cultured for one hour at 37 °C to allow stimulation and signal transmission. After one hour, cells were incubated with Golgi plug (Becton Dickinson Biosciences, Franklin Lakes, NJ) for three hours at 37 °C to block secretion of IFN-γ. Cells were then stained for the following: Viability Dye eFlour 506 (eBioscience, San Diego, CA) and antibodies for CD3 (clone 145-2C11, eBioscience), CD4 (clone RM4–5, Invitrogen), and CD8 (clone 53–6.7, eBiosciences) diluted in Fc Block (Becton Dickinson Biosciences). Cells were washed again, fixed and permeabilized using the BD Cytofix/Cytoperm kit (eBioscience), and stained for intracellular IFN-γ (clone XMG1.2, eBioscience). Experimental controls were splenocytes from naïve mice co-cultured with the above stimuli treatments. Results are obtained from one animal experiment with multiple biological replicates and with two technical replicate assays.

A stimulation assay for memory T cell formation was performed as described above, only differing by the time post-injection that splenocytes were harvested. In this experiment, mice excluded from the ELISA time course experiment, due to incomplete/unacceptable injection and low initial FIX levels (< 20% normal, see 'Animal Experiments'), were used at 210 dpi. Although precluded from the ELISA expression time course, vector exposure in these animals was confirmed by detection of low levels of transgene expression. To increase exposure to vector and vector-encoded transgenes, and potentially induce memory T cell recall responses, a portion of these mice were 'boosted' with a second virus injection seven days before the T cell stimulation assay. Groups consisted of mice exposed to PBS (naïve, $n = 1$), Ad5-Cas9-gRNA (boosted $n = 3$, un-boosted $n = 2$) or Ad5-gRNA (boosted $n = 1$, un-boosted $n = 1$). 'Boost' injections consisted of tail vein injection of 5.5×10^{10} VP/mouse. DC2.4 cells were transduced with 2000 VP/cell of either Adpk-GFP, Ad5-Cas9, or Ad5-gRNA. Separately, other DCs were fed 10 μg/mL recombinant Cas9 protein. Assay procedure and data analysis were performed as described above. Results are from one animal experiment with multiple biological replicates and with two technical replicate assays.

6.12. In situ hybridization of mFIX RNA/DNA and adenoviral DNA

Liver tissue was harvested from R333Q mice tail vein injected with 7.5×10^{10} VP of Ad5-EF1α-mFIX and either 2.5×10^{10} VP of Ad5-Cas9-gRNA ($n = 2$) or 2.5×10^{10} VP Ad5-GFP ($n = 2$) at 245 dpi (Supplemental Fig. 10). Mice were whole body perfused with 10% neutral buffered formalin in PBS, livers harvested and dissected, then fixed overnight at 4 °C. Next, the tissue was sequentially stored at 4 °C in 10%, 20%, and 30% sucrose solutions (Sigma-Aldrich) with overnight incubations in each solution concentration. Next the tissue was embedded in NEG-50 (Thermo Fisher Scientific) freezing media, then flash frozen using 2-methyl butane (Sigma-Aldrich) and liquid nitrogen. Tissue was sliced into 9-μm sections, placed on slides, and stored desiccated at −80 °C.

In situ identification of *mFIX* RNA and DNA, as well as adenoviral genomic DNA, was accomplished using oligonucleotide probes (Advanced Cell Diagnostics Inc., Newark, CA). Briefly, a series of 18- to 25-nt 'anti-sense' probes (approximately 20 oligonucleotides) were designed to tile across a 1.0-kb region of *mFIX* cDNA (nt: 401–1699) and mRNA. To detect adenoviral genomic DNA, 'sense' probes targeted a 1.0-kb region (nt: 26,389–27,424 of pAd-Easy1) of the adenovirus genome. Following cognate probe recognition and hybridization to a target molecule, a series of amplification steps were performed using amplifier probes specific to the target probe, according to manufacturer's protocol. Specificity is ensured by the assay's signal amplification premise, which requires at least two side-by-side target probes to be hybridized to a target molecule before the signal can be amplified for detection [77]. Chromogenic detection of *mFIX* DNA and RNA molecules resulted as red punctuate dots, while adenoviral DNA was detected as blue punctuate dots. Slides were counterstained with hematoxylin solution (Sigma-Aldrich) to stain nuclei. To ensure probe hybridization to DNA, a brief denaturation at 65 °C followed by overnight hybridization at 40 °C was performed [78]. DNA detection was separately confirmed by detection of signals on slides treated with RNaseA/T1 solution (Thermo Fisher Scientific). Liver sections from an untreated C57Bl/6J mouse served as a positive control for *mFIX* DNA and RNA recognition. Controls probes consisted of 2-plex negative probes targeting the bacterial gene *dapB* (one probe per detection channel), while positive probes recognized murine *PPIB* and *POLR2A*. Slides were observed and imaged using bright field microscopy.

Thirty random images of liver sections from treated mice at 40× magnification were chosen for analysis of nuclear signals of *mFIX* RNA/

DNA and adenoviral genomic DNA. Additional images for analysis included liver sections of a C57Bl/6J mouse and treated mice hybridized with negative and positive control probes. Slide images were from three independent hybridization experiments. Images were randomized and blinded for unbiased quantification of nuclei containing red *mFIX* signal, blue adenoviral genome signal, or co-localization of both signals.

6.13. Statistics

ELISA statistical analysis was performed by comparing groups at each individual time-point. To perform parametric testing, an *F*-test determined whether the groups' samples had equal variance. If equal variance was determined, a Student's *t*-test was used. For data with significantly unequal variance, a heteroskedastic *t*-test was used. To test for significance without the assumption of normal distribution, data was submitted to non-parametric Mann-Whitney *U* test. Data was only deemed significant if both parametric and non-parametric tests were in agreement. Testing was performed using the Real Stats Software package in Microsoft Excel (http://www.real-statistics.com/free-download/).

Statistical analysis of flow cytometry data was performed with unpaired Student t-test or one-way ANOVA followed by Tukey post-test comparison. All other statistical analysis was performed using GraphPad PRISM software. First, each groups' data was tested for a normal distribution using a D'Agostino Pearson Test or Shapiro-Wilk Test (if 'n' was too small for D'Agostino Pearson testing). Normally distributed data was used in parametric unpaired *t*-tests to compare groups. If groups had equal variance (determined *via F*-test) an unpaired Student's *t*-test was used. If groups had significantly different variance an unpaired *t*-test with Welch's correction was used. For comparison of non-normally distributed data, non-parametric Mann-Whitney *U* test was performed. All *t*-tests were two-tailed. For all statistical analyses *p*-values were denoted as > 0.05 (no significance [ns]), < 0.05 (*), < 0.01 (**), or < 0.001 (***).

6.14. Study approval

Animals were housed in pathogen free conditions with access to food and water *ad libitum* under guidelines and care of the Department of Comparative Medicine at WUSM. The WUSM animal management program is American Association for the Accreditation of Laboratory Animal Care accredited, and meets NIH Guide for the Care and Use of Laboratory Animals standards. All animal experiments were performed in accordance to an IACUC approved protocol (#201510191).

Ethics approval and consent to participate

Not applicable.

Consent for publication

Not applicable.

Availability of data and material

The datasets supporting the conclusions of this article are included within the article and its additional files.

Competing interests

The authors have declared that no conflict of interest exists.

Funding

This work was supported by the NIH Grants R01-CA15469, F31-DK108624, and R25-GM103757. The Siteman Cancer Center is supported in part by the NCI Cancer Center Support Grant P30-CA91842.

Acknowledgements

We thank Drs. Katherine Ponder, George Broze, and Hideyo Ugai for advice on project design and critical reading of the manuscript. We thank Dr. Shondra Miller for providing plasmids essential to this study and Dr. Paul Monahan for gifting the R333Q mouse line. We appreciate the MGC for assistance in animal husbandry and the GEiC for performing targeted deep sequencing. We also thank Mr. William Everett for assistance in statistical analysis and Amanda Baker for extensive advice on the manuscript.

Authors contributions

C.S. and D.T.C formulated and designed the project. C.S. devised and performed all experiments. E.L. and W.Y. assisted in T cell assay design and experiments. E.L aided figure generation and manuscript preparation. E.K. and Z.H.L. contributed to animal experiments. C.S., E.L., and D.T.C. assisted in data interpretation. C.S. and E.L. performed statistical analysis. C.S. and D.T.C wrote the manuscript with input from all authors.

Appendix A. Supplementary data

Supplementary data to this article can be found online at https://doi.org/10.1016/j.jconrel.2019.02.009.

References

[1] W. Miesbach, et al., Gene therapy with adeno-associated virus vector 5-human factor IX in adults with hemophilia B, Published online ahead of print December 15, Blood (2017), https://doi.org/10.1182/blood-2017-09-804419.
[2] L.A. George, et al., Hemophilia B gene therapy with a high-specific-activity factor IX variant, N. Engl. J. Med. 377 (23) (2017) 2215–2227.
[3] A.C. Nathwani, et al., Long-term safety and efficacy of factor IX gene therapy in hemophilia B, N. Engl. J. Med. 371 (21) (2014) 1994–2004.
[4] L. Wang, H. Wang, P. Bell, D. McMenamin, J.M. Wilson, Hepatic gene transfer in neonatal mice by adeno-associated virus serotype 8 vector, Hum. Gene Ther. 23 (5) (2011) 533–539.
[5] S.C. Cunningham, A.P. Dane, A. Spinoulas, I.E. Alexander, Gene delivery to the juvenile mouse liver using rAAV2/8 vectors, Mol. Ther. 16 (6) (2008) 1081–1088.
[6] C. Hu, R.G. Cela, M. Suzuki, B. Lee, G.S. Lipshutz, Neonatal helper-dependent adenoviral vector gene therapy mediates correction of hemophilia a and tolerance to human factor VIII, Proc. Natl. Acad. Sci. U. S. A. 108 (5) (2011) 2082–2087.
[7] L. Wang, P. Bell, J. Lin, R. Calcedo, A.F. Tarantal, J.M. Wilson, rAAV8-mediated hepatic gene transfer in infant rhesus monkeys (*Macaca mulatta*), Mol. Ther. 19 (11) (2011) 2012–2020.
[8] S. Hacein-Bey-Abina, et al., A modified γ-retrovirus vector for X-linked severe combined immunodeficiency, N. Engl. J. Med. 371 (15) (2014) 1407–1417.
[9] F. Candotti, et al., Gene therapy for adenosine deaminase-deficient severe combined immune deficiency: clinical comparison of retroviral vectors and treatment plans, Published online September 11, Blood (2012), https://doi.org/10.1182/blood-2012-02-400937.
[10] U. Modlich, et al., Insertional transformation of hematopoietic cells by self-inactivating lentiviral and gammaretroviral vectors, Mol. Ther. 17 (11) (2009) 1919–1928.
[11] C.J. Braun, et al., Gene therapy for Wiskott-Aldrich syndrome—long-term efficacy and genotoxicity, Sci. Transl. Med. 6 (227) (2014) 227ra33.
[12] D. Cesana, et al., Uncovering and dissecting the genotoxicity of self-inactivating lentiviral vectors in vivo, Mol. Ther. 22 (4) (2014) 774–785.
[13] W. Xu, J.L. Russ, M.V. Eiden, Evaluation of residual promoter activity in γ-retroviral self-inactivating (SIN) vectors, Mol. Ther. 20 (1) (2012) 84–90.
[14] H. Li, et al., In vivo genome editing restores haemostasis in a mouse model of haemophilia, Nature 475 (7355) (2011) 217–221.
[15] T. Ohmori, et al., CRISPR/Cas9-mediated genome editing via postnatal administration of rAAV vector cures haemophilia B mice, Sci. Rep. 7 (1) (2017) 4159.
[16] C. Huai, et al., CRISPR/Cas9-mediated somatic and germline gene correction to restore hemostasis in hemophilia B mice, Hum. Genet. 136 (7) (2017) 875–883.
[17] A. Barzel, et al., Promoterless gene targeting without nucleases ameliorates haemophilia B in mice, Nature 517 (7534) (2015) 360–364.
[18] U.S. National Library of Medicine, Clinical Trials Web Site, https://clinicaltrials.gov/ct2/show/NCT02695160 Updated March 30, 2018. Accessed August 2, 2018.
[19] C.N.Z. Mattar, et al., In utero transfer of adeno-associated viral vectors produces long-term factor IX levels in a cynomolgus macaque model, Mol. Ther. 25 (8)

(2017) 1843–1853.
[20] A. Donsante, et al., rAAV vector integration sites in mouse hepatocellular carcinoma, Science 317 (5837) (2007) 477.
[21] R.J. Chandler, M.S. Sands, C.P. Venditti, Recombinant adeno-associated viral integration and genotoxicity: insights from animal models, Hum. Gene Ther. 28 (4) (2017) 314–322.
[22] L. Wang, et al., Meganuclease targeting of PCSK9 in macaque liver leads to stable reduction in serum cholesterol, Nat. Biotechnol. 36 (8) (2018) 717–725.
[23] T. Bergmann, et al., Designer nuclease-mediated gene correction via homology-directed repair in an in vitro model of canine hemophilia B, J. Genet. Med. 20 (5) (2018) 3020.
[24] I. Maggio, M. Holkers, J. Liu, J.M. Janssen, X. Chen, M.A. Gonçalves, Adenoviral vector delivery of RNA-guided CRISPR/Cas9 nuclease complexes induces targeted mutagenesis in a diverse array of human cells, Sci. Rep. 4 (2014) 5105.
[25] O. Voets, et al., Highly efficient gene inactivation by adenoviral CRISPR/Cas9 in human primary cells, PLoS One 12 (8) (2017) e0182974.
[26] M. Richter, et al., In vivo transduction of primitive mobilized hematopoietic stem cells after intravenous injection of integrating adenovirus vectors, Blood 128 (2016) 2206–2217.
[27] D.J. Palmer, N.C. Grove, D.L. Turner, P. Ng, Gene editing with helper-dependent adenovirus can efficiently introduce multiple changes simultaneously over a large genomic region, Mol. Ther. Nucleic Acids 8 (2017) 101–110.
[28] S.L. Stephen, et al., Chromosomal integration of adenoviral vector DNA in vivo, J. Virol. 84 (2010) 9987–9994.
[29] C.J. Stephens, E. Kashentseva, W. Everett, L. Kaliberova, D.T. Curiel, Targeted in vivo knock-in of human alpha-1-antitrypsin cDNA using adenoviral delivery of CRISPR/Cas9, Gene Ther. 25 (2) (2018) 139–156.
[30] T.I. Cornu, C. Mussolino, T. Cathomen, Refining strategies to translate genome editing to the clinic, Nat. Med. 23 (4) (2017) 415–423.
[31] M. Holkers, et al., Adenoviral vector DNA for accurate genome editing with engineered nucleases, Nat. Methods 11 (10) (2014) 1051–1057.
[32] W.L. Chew, et al., A multifunctional rAAV–CRISPR–Cas9 and its host response, Nat. Methods 13 (10) (2016) 868–874.
[33] D. Wang, et al., Adenovirus-mediated somatic genome editing of Pten by CRISPR/Cas9 in mouse liver in spite of Cas9-specific immune responses, Hum. Gene Ther. 26 (7) (2015) 432–442.
[34] M.A. Kay, et al., In vivo hepatic gene therapy: complete albeit transient correction of factor IX deficiency in hemophilia B dogs, Proc. Natl. Acad. Sci. U. S. A. 91 (6) (1994) 2353–2357.
[35] D. Maione, et al., An improved helper-dependent adenoviral vector allows persistent gene expression after intramuscular delivery and overcomes preexisting immunity to adenovirus, Proc. Natl. Acad. Sci. U. S. A. 98 (11) (2001) 5986–5991.
[36] N. Dronadula, B.K. Wacker, R. Van Der Kwast, J. Zhang, D.A. Dichek, Stable in vivo transgene expression in endothelial cells with helper-dependent adenovirus: roles of promoter and interleukin-10, Hum. Gene Ther. 28 (3) (2017) 255–270.
[37] S. Iizuka, F. Sakurai, M. Tachibana, K. Ohashi, H. Mizuguchi, Neonatal gene therapy for hemophilia B by a novel adenovirus vector showing reduced leaky expression of viral genes, Mol. Ther. Methods Clin. Dev. 6 (2017) 183–193.
[38] M.A. Kay, F. Graham, F. Leland, S.L. Woo, Therapeutic serum concentrations of human alpha-1-antitrypsin after adenoviral-mediated gene transfer into mouse hepatocytes, Hepatology 21 (3) (1995) 815–819.
[39] A. Ehrhardt, X. Hui, M.A. Kay, Episomal persistence of recombinant adenoviral vector genomes during the cell cycle in vivo, J. Virol. 77 (13) (2003) 7689–7695.
[40] F. Kreppel, S. Kochanek, Long-term transgene expression in proliferating cells mediated by episomally maintained high-capacity adenovirus vectors, J. Virol. 78 (1) (2004) 9–22.
[41] S. Dutta, P. Sengupta, Men and mice: relating their ages, Life Sci. 152 (2016) 244–248.
[42] Y. Malato, et al., Fate tracing of mature hepatocytes in mouse liver homeostasis and regeneration, J. Clin. Invest. 121 (12) (2011) 4850–4860.
[43] K. Singh, et al., Efficient in vivo liver-directed gene editing using CRISPR/Cas9, Mol. Ther. 26 (5) (2018) 1241–1254.
[44] J.D. Finn, et al., A single administration of CRISPR/Cas9 lipid nanoparticles achieves robust and persistent in vivo genome editing, Cell Rep. 22 (9) (2018) 2227–2235.
[45] Y. Yang, et al., A dual rAAV system enables the Cas9-mediated correction of a metabolic liver disease in newborn mice, Nat. Biotechnol. 34 (3) (2016) 334–338.
[46] T. Sakuma, K. Mochida, S. Nakade, T. Ezure, S. Minagawa, T. Yamamoto, Unexpected heterogeneity derived from Cas9 ribonucleoprotein-introduced clonal cells at the HPRT 1 locus, Genes Cells 23 (4) (2018) 255–263.
[47] P. Verma, R.A. Greenberg, Noncanonical views of homology-directed DNA repair, Genes Dev. 30 (10) (2016) 1138–1154.
[48] F. Adikusuma, et al., Large deletions induced by Cas9 cleavage, Nature 560 (7717) (2018) E8–E9.
[49] M. Kosicki, K. Tomberg, A. Bradley, Repair of double-strand breaks induced by CRISPR–Cas9 leads to large deletions and complex rearrangements, Published online ahead of print July 16, Nat. Biotechnol. (2018), https://doi.org/10.1038/nbt.4192.
[50] C.E. Thomas, A. Ehrhardt, M.A. Kay, Progress and problems with the use of viral vectors for gene therapy, Nat. Rev. Genet. 4 (5) (2003) 346–358.
[51] E. Riu, Z.Y. Chen, H. Xu, C.Y. He, M.A. Kay, Histone modifications are associated with the persistence or silencing of vector-mediated transgene expression in vivo, Mol. Ther. 15 (7) (2007) 1348–1355.
[52] Y. Yang, et al., Cellular immunity to viral antigens limits E1-deleted adenoviruses for gene therapy, Proc. Natl. Acad. Sci. U. S. A. 91 (10) (1994) 4407–4411.
[53] S. Atasheva, D.M. Shayakhmetov, Adenovirus sensing by the immune system, Curr. Opin. Virol. 21 (2016) 109–113.
[54] C.T. Charlesworth, et al., Identification of pre-existing adaptive immunity to Cas9 proteins in humans, Published online ahead of print January 5, BioRxiv (2018), https://doi.org/10.1101/243345.
[55] V.L. Simhadri, J. McGill, S. McMahon, J. Wang, H. Jiang, Z.E. Sauna, Prevalence of pre-existing antibodies to CRISPR-associated nuclease Cas9 in the US population, Mol. Ther. Methods Clin. Dev. 10 (1) (2018) 105–112.
[56] B. Wienert, J. Shin, E. Zelin, K. Pestal, J.E. Corn, In vitro–transcribed guide RNAs trigger an innate immune response via the RIG-I pathway, PLoS Biol. 16 (7) (2018) e2005840.
[57] Kim S, et al. CRISPR RNAs trigger innate immune responses in human cells. Genome Res. doi:https://doi.org/10.1101/gr.231936.11.
[58] P. Penaloza-MacMaster, et al., Inhibitory receptor expression on memory CD8 T cells following ad vector immunization, Vaccine 34 (4) (2016) 4955–4963.
[59] D.L. Wagner, L. Amani, D.J. Wendering, P. Reinke, H.D. Volk, M. Schmueck-Henneresse, High prevalence of S. Pyogenes Cas9-specific T cell sensitization within the adult human population-a balanced effector/regulatory T cell response, Published online ahead of print October 29, Nat. Med. (2018), https://doi.org/10.1038/s41591-018-0204-6.
[60] A. Rahman, et al., Specific depletion of human anti-adenovirus antibodies facilitates transduction in an in vivo model for systemic gene therapy, Mol. Ther. 3 (5) (2001) 768–778.
[61] D.A. Muruve, M.J. Barnes, I.E. Stillman, T.A. Libermann, Adenoviral gene therapy leads to rapid induction of multiple chemokines and acute neutrophil-dependent hepatic injury in vivo, Hum. Gene Ther. 10 (6) (1999) 965–976.
[62] A. Lieber, C.Y. He, L. Meuse, D. Schowalter, I. Kirillova, B. Winther, M.A. Kay, The role of Kupffer cell activation and viral gene expression in early liver toxicity after infusion of recombinant adenovirus vectors, J. Virol. 71 (11) (1997) 8798–8807.
[63] A.S. Ricciardi, et al., In utero nanoparticle delivery for site-specific genome editing, Nat. Commun. 9 (1) (2018) 2481.
[64] Y. Guan, et al., CRISPR/Cas9-mediated somatic correction of a novel coagulator factor IX gene mutation ameliorates hemophilia in mouse, EMBO Mol. Med. 8 (5) (2016) 477–488.
[65] F. Mingozzi, et al., Induction of immune tolerance to coagulation factor IX antigen by in vivo hepatic gene transfer, J. Clin. Invest. 111 (9) (2003) 1347–1356.
[66] P.E. Monahan, et al., Employing a gain-of-function factor IX variant R338L to advance the efficacy and safety of hemophilia B human gene therapy: preclinical evaluation supporting an ongoing adeno-associated virus clinical trial, Hum. Gene Ther. 26 (2) (2014) 69–81.
[67] L. Graf, Extended half-life factor VIII and factor IX preparations, Transfus. Med. Hemother. 45 (2) (2018) 86–91.
[68] I. Wilkinson-Ryan, et al., Incorporation of porcine adenovirus 4 fiber protein enhances infectivity of adenovirus vector on dendritic cells: implications for immune-mediated cancer therapy, PLoS One 10 (5) (2015) e0125851.
[69] H. Ugai, et al., In vitro dynamic visualization analysis of fluorescently labeled minor capsid protein IX and core protein V by simultaneous detection, J. Mol. Biol. 395 (1) (2010) 55–78.
[70] C. Chartier, E. Degryse, M. Gantzer, A. Dieterle, A. Pavirani, M. Mehtali, Efficient generation of recombinant adenovirus vectors by homologous recombination in *Escherichia coli*, J. Virol. 70 (7) (1996) 4805–4810.
[71] D.Y. Jin, T.P. Zhang, T. Gui, D.W. Stafford, P.E. Monahan, Creation of a mouse expressing defective human factor IX, Blood 104 (6) (2004) 1733–1739.
[72] C.A. Maguire, et al., Mouse gender influences brain transduction by intravascularly administered rAAV9, Mol. Ther. 21 (8) (2013) 1470–1471.
[73] M. Schmidt, et al., High-resolution insertion-site analysis by linear amplification–mediated PCR (LAM-PCR), Nat. Methods 4 (12) (2007) 1051–1057.
[74] G.M. Boratyn, et al., BLAST: a more efficient report with usability improvements, Nucleic Acids Res. 41 (W1) (2013) W29–W33.
[75] R.W.H. Ruigrok, M.V. Nermut, P.J. Andree, The molecular mass of adenovirus type 5 as determined by means of scanning transmission electron microscopy (STEM), J. Virol. Methods 9 (1) (1984) 69–78.
[76] E.J. Lauron, L. Yang, J.I. Elliott, M.D. Gainey, D.H. Fremont, W.M. Yokoyama, Cross-priming induces immunodomination in the presence of viral MHC class I inhibition, PLoS Pathog. 14 (2) (2018) e1006883.
[77] F. Wang, et al., RNAscope: a novel in situ RNA analysis platform for formalin-fixed, paraffin-embedded tissues, J. Mol. Diagn. 14 (1) (2012) 22–29.
[78] C. Deleage, et al., Defining HIV and SIV reservoirs in lymphoid tissues, Pathol. Immun. 1 (1) (2016) 68–105.